

Statistical relationships between biological parameters and environmental forcings in Lake Erie, 1970s–2010s

Hongyan Zhang¹, Jia Wang², Ting-yi Yang^{2,3}, Brent Lofgren², and Philip Chu²

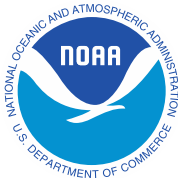
¹ Cooperative Institute for Great Lakes Research, University of Michigan

² NOAA Great Lakes Environmental Research Laboratory, Ann Arbor, Michigan

³ Geodetic Science, School of Earth Science, the Ohio State University, Columbus, Ohio

NOAA Great Lakes Environmental Research Laboratory
4840 S. State Road, Ann Arbor, Michigan

Monday, October 29, 2018



UNITED STATES
DEPARTMENT OF COMMERCE

Wilbur L. Ross, Jr., Secretary

NATIONAL OCEANIC AND
ATMOSPHERIC ADMINISTRATION

RDML Tim Gallaudet, Ph.D., USN Ret.,
Acting Administrator

NOTICE

Mention of a commercial company or product does not constitute an endorsement by the NOAA. Use of information from this publication concerning proprietary products or the tests of such products for publicity or advertising purposes is not authorized. This is GLERL Contribution No. 1901 and CIGLR Contribution No. 1134.

This publication is available as a PDF file and can be downloaded from GLERL's web site: www.glerl.noaa.gov or by emailing GLERL Information Services at oar.pubs.glerl@noaa.gov.

TABLE of CONTENTS

ABSTRACT.....	7
1.0 INTRODUCTION	7
2.0 DATA SETS DESCRIPTION	8
2.1 Biological parameters	8
2.2 Environmental forcings.....	9
3.0 DEFINITION AND METHODOLOGY	10
4.0 RESULTS	13
4.1 Correlation between environmental forcings and biological parameters.....	13
4.2 Linear regression between environmental forcings and biological parameters	31
5.0 SUMMARY	60
6.0 ACKNOWLEDGMENTS	60
7.0 REFERENCES	61
8.0 APPENDIX: LAKE ERIE BIOLOGICAL PARAMETERS AND ENVIRONMENTAL FORCINGS.....	63

LIST of FIGURES

Figure 1. Distribution of air temperature stations. (Annotated number denotes percentage of the data coverage).	11
Figure 2. Linear correlation between Lake Erie AMIC and biological parameters.....	14
Figure 3. Linear correlation between entire Great Lakes AMIC and biological parameters.....	15
Figure 4. Linear correlation between ENSO and biological parameters.	16
Figure 5. Correlation between ENSO ² and biological parameters.	17
Figure 6. Correlation between NAO and biological parameters.....	18
Figure 7. Correlation between NAO ² and biological parameters.	19
Figure 8. Correlation between PDO and biological parameters.	20
Figure 9. Correlation between PDO ² and biological parameters.....	21
Figure 10. Linear correlation between AMO and biological parameters.	22
Figure 11. Correlation between AMO ² (quadratic or nonlinear) and biological parameters.....	23
Figure 12. Correlation between ice duration and biological parameters.	24
Figure 13. Correlation between WSI and biological parameters.	25
Figure 14. Correlation between spring water temperature and biological parameters.	26
Figure 15. Correlation between summer water temperature and biological parameters.	27
Figure 16. Correlation between wind speed and biological parameters.	28
Figure 17. Correlation between wind speed squared (quadratic; equivalent to wind stress) and biological parameters.	29
Figure 18. Correlation between wind speed cubed (equivalent to wind mixing) and biological parameters.	30
Figure 19. Regression between diatom in April and four atmospheric teleconnection patterns. .	32
Figure 20. Regression between diatom in April and other physical forcings.	33
Figure 21. Regression between diatom in April and wind speed, its quadratic and cubed forms.	34
Figure 22. Regression between diatom in April and other biological parameters.	35
Figure 23. Regression between HOD and four teleconnection patterns.	36
Figure 24. Regression between HOD and other physical forcings.	37
Figure 25. Regression between HOD and wind speed, its quadratic and cubed forms.	38
Figure 26. Regression between HOD and other biological parameters.	39
Figure 27. Regression between maximum hypoxia area and four teleconnection patterns.....	40
Figure 28. Regression between maximum hypoxia area and other physical forcings.....	41
Figure 29. Regression between maximum hypoxia area and wind speed, its quadratic and cubed forms.	42
Figure 30. Regression between maximum hypoxia area and other biological parameters.	43
Figure 31. Regression between mean hypoxia area and four teleconnection patterns.	44
Figure 32. Regression between mean hypoxia area and other physical forcings.	45
Figure 33. Regression between mean hypoxia area and wind speed, its quadratic and cubed forms.	46
Figure 34. Regression between mean hypoxia area and other biological parameters.	47
Figure 35. Regression between mean dissolved oxygen and four teleconnection patterns.	48
Figure 36. Regression between mean dissolved oxygen and other physical forcings.	49
Figure 37. Regression between mean dissolved oxygen and wind speed, its quadratic and cubed forms.	50
Figure 38. Regression between mean dissolved oxygen and other biological parameters.	51
Figure 39. Regression between median dissolved oxygen and four teleconnection patterns.	52

Figure 40. Regression between median dissolved oxygen and other physical forcings.	53
Figure 41. Regression between median dissolved oxygen and wind speed, its quadratic and cubed forms.....	54
Figure 42. Regression between median dissolved oxygen and other biological parameters.	55
Figure 43. Regression between river phosphate load and four teleconnection patterns.	56
Figure 44. Regression between river phosphate load and other physical forcings.	57
Figure 45. Regression between river phosphate load and wind speed, its quadratic and cubed forms.	58
Figure 46. Regression between river phosphate load and other biological forcings.	59

LIST of TABLES

Table 1. List of selected meteorological stations	12
Table 2. Time series of environmental/physical forcings.	64
Table 3. Time series of biological parameters.	65
Table 4. Time series of teleconnection pattern indices.	67
Table 5. Correlation coefficients between environmental/physical forcings and biological parameters. The bolded coefficients are at the 95% significance level.	68
Table 6. Correlation coefficients between biological parameters. The bolded coefficients are at the 95% significance level.	68
Table 7. Summary of the long-term trend [$y=a+b(t-T_0)$, where t is time in year] of each parameter and some important statistics of the long-term changes.	69

Statistical relationships between biological parameters and environmental forcings in Lake Erie, 1970s–2010s

Hongyan Zhang, Jia Wang, Ting-yi Yang, Brent Lofgren, and Philip Chu

ABSTRACT

This report investigates interannual variability of biological parameters (diatom, hypoxia area, hypolimnetic oxygen depletion, dissolved oxygen, and phosphate load) and related environmental forcings (annual maximum ice cover, ice duration, wind speed, lake temperature, winter severity index, and four teleconnection patterns: El Niño-Southern Oscillation (ENSO), North Atlantic oscillation (NAO), Pacific Decadal Oscillation (PDO), and Atlantic Multidecadal Oscillation (AMO)). The statistical relationships are examined between two variables. Scatter and linear/non-linear regression methods are used to determine whether they have linear or quadratic (non-linear) relationships. The purpose of this report is to 1) provide users with Lake Erie biological parameters and environmental forcings in as simple as possible format of graphs and tables; 2) explore the possible relationship between a single pair of parameters that are easily digested and applied to resources management, projection, and planning; and 3) lay a foundation towards the construction of multi-variable regression models to hindcast the retrospective measurements and to project seasonal variations of hypoxia and other biological parameters using physical/climate forcings as predictors.

1.0 INTRODUCTION

The Laurentian Great Lakes, located in the mid-latitude of eastern North America, contain about 95% of the United States' and 20% of the world's fresh surface water supply. Nearly one eighth of the population of the United States and one third of the population of Canada live within their drainage basins. The Great Lakes can be considered a mini climate system—though small compared to the global climate system or Arctic regional climate system—since all five important climate components are included: regional atmosphere and climate, hydrosphere (hydrodynamics), cryosphere (lake ice), biosphere (aquatic ecosystem and terrestrial ecosystem), and land process (hydrology). In addition, the human dimension is another important component affecting the Great Lakes climate system. In this mini-climate system, there are strong interactions and associations among the components. Because of this concentration of population (human dimension), the ice cover that forms on the Great Lakes each winter, and its year-to-year variability, affect the regional economy (Niim, 1982). It also affects the lake's abiotic environment and ecosystems (Vanderploeg et al. 1992), and therefore influences summer hypoxia, lake effect snow, water level variability, and the overall hydrologic cycle of the region (Assel et al. 2004).

Studies show that atmospheric teleconnection patterns such as the North Atlantic Oscillation (NAO), El Niño and Southern Oscillation (ENSO) (Bai et al. 2012), Pacific Decadal Oscillation

(PDO), and Atlantic Multidecadal Oscillation (AMO) are associated with anomalous ice cover on the Great Lakes (Wang et al. 2018). Mishra et al. (2011) also shows that lake ice phenology of small lakes around the Great Lakes region is associated with these major climate teleconnection patterns.

Hypoxia ($DO < 2$ mg/L) is a worldwide eutrophication problem. Hypoxia occurs when water is stable with high oxygen demand due to organic matter decomposition and chemical oxidation processes at the bottom of a water, especially in the hypolimnion of thermal stratified waters during warm seasons. Thus, hypoxia is affected by both physical and biological conditions. The central basin of Lake Erie experiences historical hypoxia, but the hypoxia tends to increase in area extent and duration in recent years (Scavia et al. 2014). In a hypoxia retrospective statistical analysis, Zhou et al. (2015) found that river discharge to Lake Erie from April to June was a variable with the highest explanatory power. However, contradictory to understanding that high river discharge would result in high productivity, and consequently lead to large hypoxia extent, the river discharge was negatively related to hypoxia extent. Zhou et al. (2015) attributed this to some meteorological conditions that correlated with discharge but were not represented in the candidate variables examined. Climate change is predicted to increase nutrient loads, biological productivity, and water temperature, which may all enhance hypoxia in Lake Erie (Michalak et al. 2013). This report documents time series data of hypoxia indices and some important physical and biological parameters, especially atmospheric teleconnection patterns. Some preliminary statistical analyses are conducted and presented.

2.0 DATA SETS DESCRIPTION

2.1 Biological parameters

2.1-1 *Diatom (or spring chlorophyll a)*

Spring chlorophyll a in the western basin of Lake Erie were extracted from the U.S. EPA Great Lakes Environmental Database (GLENDa; <https://cdx.epa.gov/>), and averaged over all sampling stations and across spring months (January, February, March, and April) for each sampling year.

2.1-2 *HOD (hypolimnetic oxygen depletion)*

The HOD time series were taken from Great Lakes National Program Office, U.S. EPA (Watson et al., 2016)

2.1-3 *Hypoxia area*

Maximum hypoxic area and mean hypoxic area were from Zhou et al. (2015) and Del Giudice et al. (2018).

2.1-4 *Dissolved oxygen (DO)*

Bottom dissolved oxygen were extracted from the U.S. EPA Great Lakes Environmental Database (GLENDa; <https://cdx.epa.gov/>). Mean and median DO for each year were calculated based on samples in August.

2.1-5 Phosphate load

Annual total phosphate loads were taken from Dolan and Chapra (2012) and Maccoux et al. (2016).

2.2 Environmental forcings

2.2-1 Ice coverage data

The ice coverage ASCII gridded data is provided by the National Ice Center (NIC: https://www.natice.noaa.gov/products/great_lakes.html) from November 1972 until Jun 2018. Before May 2007, the ice data was mapped with Mercator projection (Clarke 1866 ellipsoid) and re-sampled to a 510 x 516 pixels gridded data. Since November 2007, the data was changed to 1024 x 1024 pixels grid (with Mercator projection and WGS 1984 ellipsoid), to improve the resolution from 2.55 km to 1.275 km (Wang et al., 2012; Wang et al., 2017). In our process, the ice coverage data is averaged at each lake, so resampling method was not used for data before the winter of 2008.

2.2-2 Air temperature data

Global Historical Climate Network Daily (GHCND; <https://www.ncdc.noaa.gov/gHCN-daily-description>) long-term daily air temperature data was used. The pre-processing and data cleaning was done and organized by Hunter et al. (2015). In our process, maximum and minimum temperature are utilized, because most of the stations do not have long-term averaged temperature. Therefore, averaged maximum and minimum temperature was used instead of averaged temperature. Because there are around 700 stations around the Great Lakes, we set up some criteria to select the most useful stations:

- A. Stations within 50km outside the lake's basin.
- B. Time span includes 1973 – 2018.
- C. Data coverage (observation over a period of observed time) is more than 90%. However, some regions do not have enough stations, e.g. north side of Lake Superior, therefore, a few low data coverage stations are included for better station distribution.

The station locations are shown in Fig. 1 and the detailed information is listed in Table 1.

2.2-3 Atmospheric teleconnection indices (see Wang et al., 2018)

- A. ENSO: The 3-month running mean of ERSST.v3 (Extended Reconstructed Sea Surface Temperature Version 3) SST anomalies in the Niño3.4 region (5°N-5°S, 120°-170°W). Data is obtained from the NOAA/CPC (Climate Prediction Center, http://origin.cpc.ncep.noaa.gov/products/analysis_monitoring/ensostuff/ONI_change.shtml).
- B. NAO: The normalized sea level pressure difference between Azores and Iceland. Record was obtained from the Climatic Research Unit, UK (<https://crudata.uea.ac.uk/cru/data/nao/>).
- C. PDO: The standardized principal component time series of leading empirical orthogonal function (EOF) of monthly sea surface temperature anomalies (SSTA) over the North Pacific (poleward of 20° N) after the global mean SST has been removed. The PDO index is derived from <http://research.jisao.washington.edu/pdo/PDO.latest>; <https://www.ncdc.noaa.gov/teleconnections/pdo>.

- D. AMO: Defined from the patterns of SST variability in the North Atlantic once any linear trend has been removed. The AMO index is obtained from <http://www.esrl.noaa.gov/psd/data/timeseries/AMO>.

3.0 DEFINITION AND METHODOLOGY

- A. Ice coverage: freeze-up date, break-up date, duration, and AMIC.

Freeze-up and break-up date: Compute the mean for each lake and all Great Lakes area per data, and assign the free-up date and break-up date if this is the first/last date when the mean greater than or equal to 10%. NA is assigned if the mean of ice coverages are all less than 10% in that year.

Duration: Subtract the freeze-up date by the break-up date. Duration is assigned to 1 if the freeze-up and break-up date are same.

AMIC (Annual maximum ice coverage): The greatest daily percent of surface area of a lake covered by ice each winter for the Great Lakes.

- B. Air temperature: WSI.

WSI (Weather Stress Index): Developed by C. R. Snider in an earlier study, to define the Great Lakes winter severity. It is defined as average of the monthly-mean temperatures from November 1st through February 28th (or 29th for leap year) (Bai et al., 2011).

- C. Atmospheric teleconnections (ENSO, NAO, PDO, and AMO) are used to correlate with air temperature and ice coverage parameters.

Table 1. List of selected meteorological stations

Region	Station ID	Latitude (deg)	Longitude (deg)	First Year	Last year	Data Coverage (%)
Superior	CA006049443	48.3667	-89.1167	1967	2018	54
	USC00205690	46.4122	-86.6625	1911	2018	95
	USC00208043	46.6014	-85.2239	1968	2018	93
	USC00213282	47.7517	-90.3283	1913	2018	85
	USC00474953	46.7781	-90.7653	1944	2018	96
	USC00472889	46.4856	-92.2875	1963	2018	93
	USW00014858	47.1686	-88.4889	1948	2018	81
Michigan	USC00116616	41.4947	-87.6803	1952	2018	99
	USC00201896	45.6414	-85.0142	1969	2018	98
	USC00205065	44.2114	-86.2939	1888	2018	92
	USC00207690	42.4014	-86.2825	1895	2018	93
	USC00478905	45.3583	-86.8911	1944	2018	99
	USW00014839	42.9550	-87.9044	1938	2018	100
	USW00014840	43.1711	-86.2367	1896	2018	100
	USW00014850	44.7408	-85.5825	1896	2018	100
	USW00014898	44.4983	-88.1111	1886	2018	100
Huron	CA006111769	44.6333	-79.5333	1971	2018	93
	CA006117684	44.4000	-79.6333	1973	2018	99
	CA006124127	44.1667	-81.6167	1872	2018	36
	USC00201492	45.6528	-84.4725	1891	2018	93
	USC00200417	43.8081	-82.9939	1925	2018	98
	USC00206680	42.9750	-82.4194	1933	2018	97
	USW00014814	45.0606	-83.4281	1948	2018	98
	USW00014845	43.5331	-84.0797	1898	2018	100
	USW00014847	46.4794	-84.3572	1931	2018	100
Erie	CA006134190	42.0500	-82.6667	1968	2018	98
	CA006135583	42.5167	-81.6333	1957	2018	99
	CA006136606	42.8833	-79.2500	1964	2018	97
	USC00336389	41.7525	-81.2956	1950	2018	99
	USW00014846	41.4500	-82.7167	1936	2018	97
	USW00014860	42.0800	-80.1825	1926	2018	100
Ontario	CA006155878	43.8667	-78.8333	1969	2018	97
	CA006158733	43.6833	-79.6333	1937	2018	99
	CA006150689	44.1500	-77.4000	1866	2018	73
	USC00304844	43.1878	-78.6092	1893	2018	83
	USC00306314	43.4622	-76.4933	1926	2018	100
	USW00014768	43.1167	-77.6767	1926	2018	100
	USW00094790	43.9922	-76.0217	1949	2018	100
St.Clair	USW00014804	42.6083	-82.8183	1896	2018	94
	USW00014822	42.4092	-83.0100	1948	2018	100
	USC00203477	42.4078	-82.8892	1950	2018	99

4.0 RESULTS

4.1 Correlation between environmental forcings and biological parameters

This section presents the original time series of year-to-year variations and the correlations between the physical/environmental forcings (including the four teleconnection pattern indices) and biological parameters. Both linear correlation coefficients and the 95% significance level (p value <0.05) are given.

In the correlation between the teleconnection patterns and the biological parameters, we also calculate the correlation between the squared index and the biological parameters to investigate the possible non-linear (quadratic) relationship.

In a similar manner, in addition to wind speed (force) alone, we also use the squared and cubed wind speed, representing the impact of wind stress (squared wind speed) and wind-induced wave mixing (cubed wind speed) (Hu and Wang 2012) on biological parameters. The results indicate that both squared and cubed wind speed have comparable correlation with the biological parameters as wind speed alone.

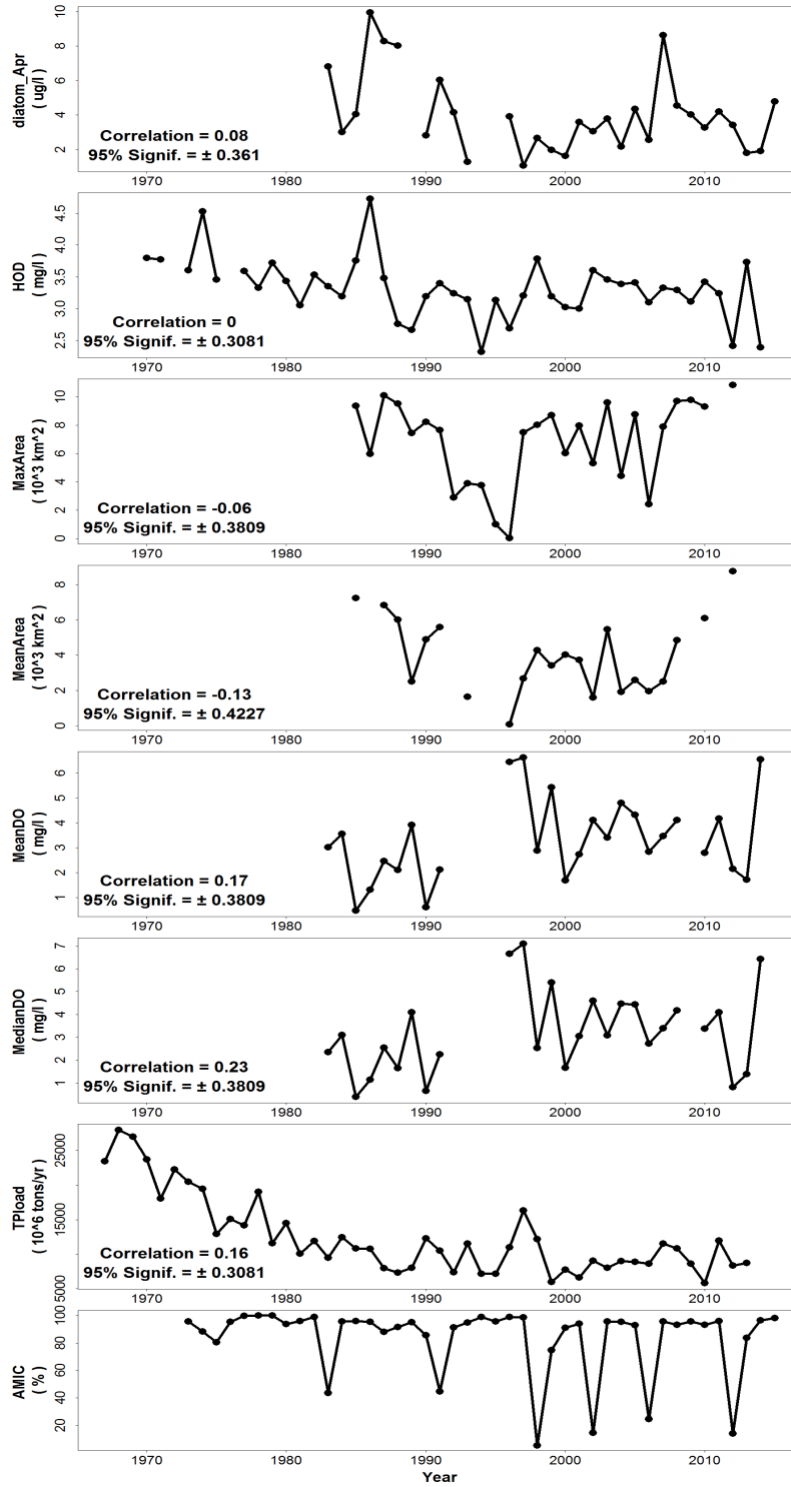


Figure 2. Linear correlation between Lake Erie AMIC and biological parameters.

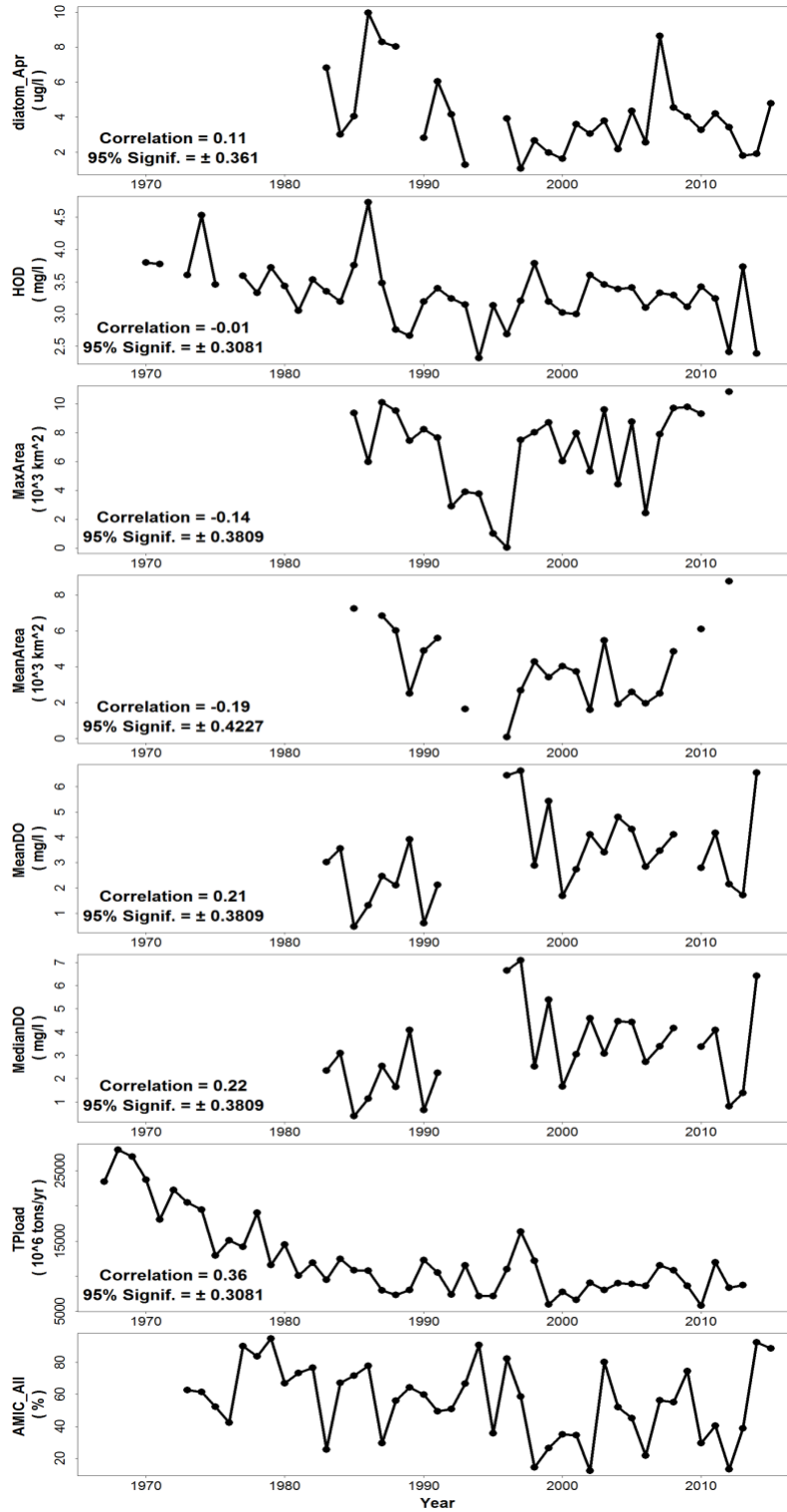


Figure 3. Linear correlation between entire Great Lakes AMIC and biological parameters.

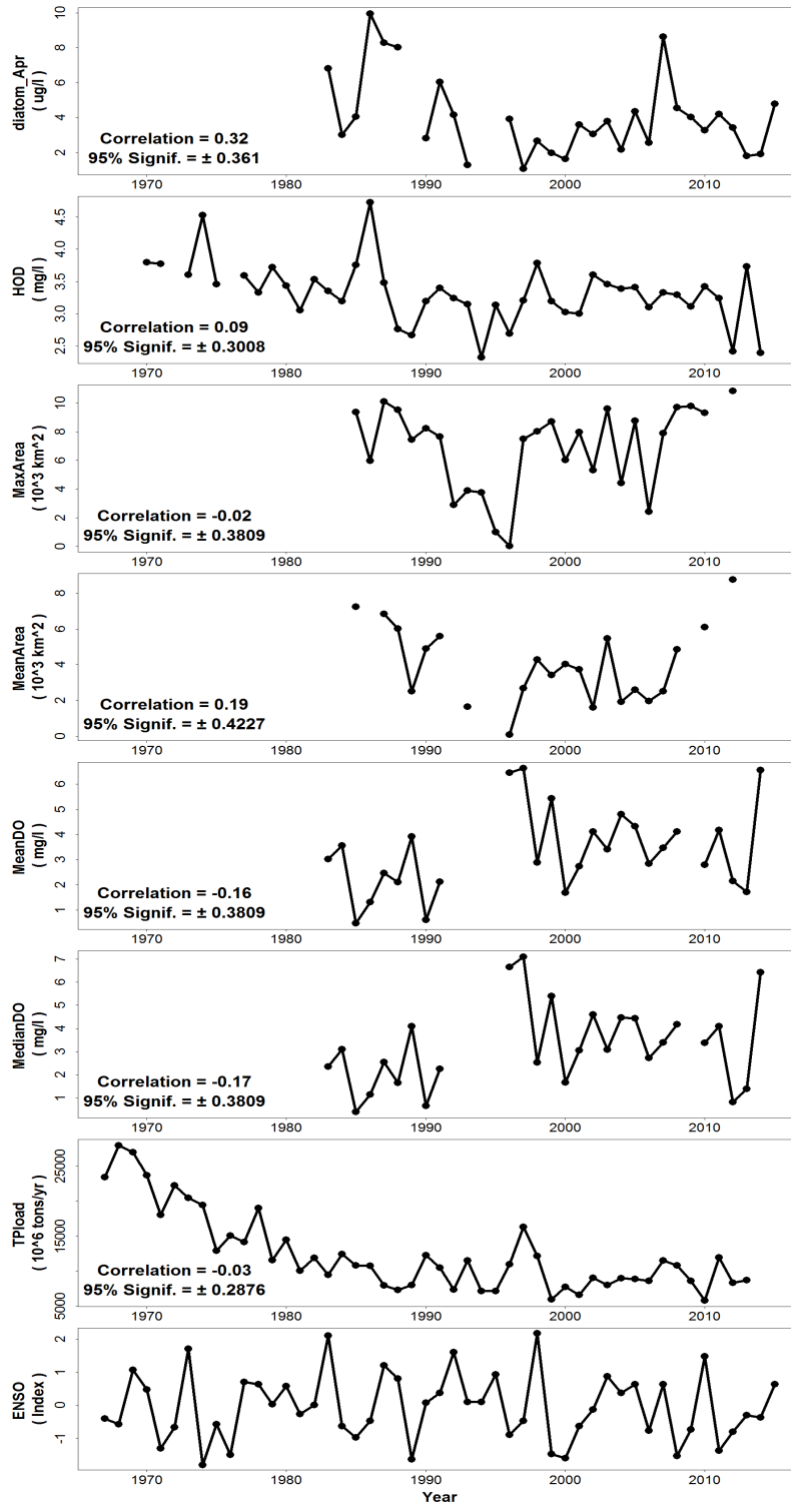


Figure 4. Linear correlation between ENSO and biological parameters.

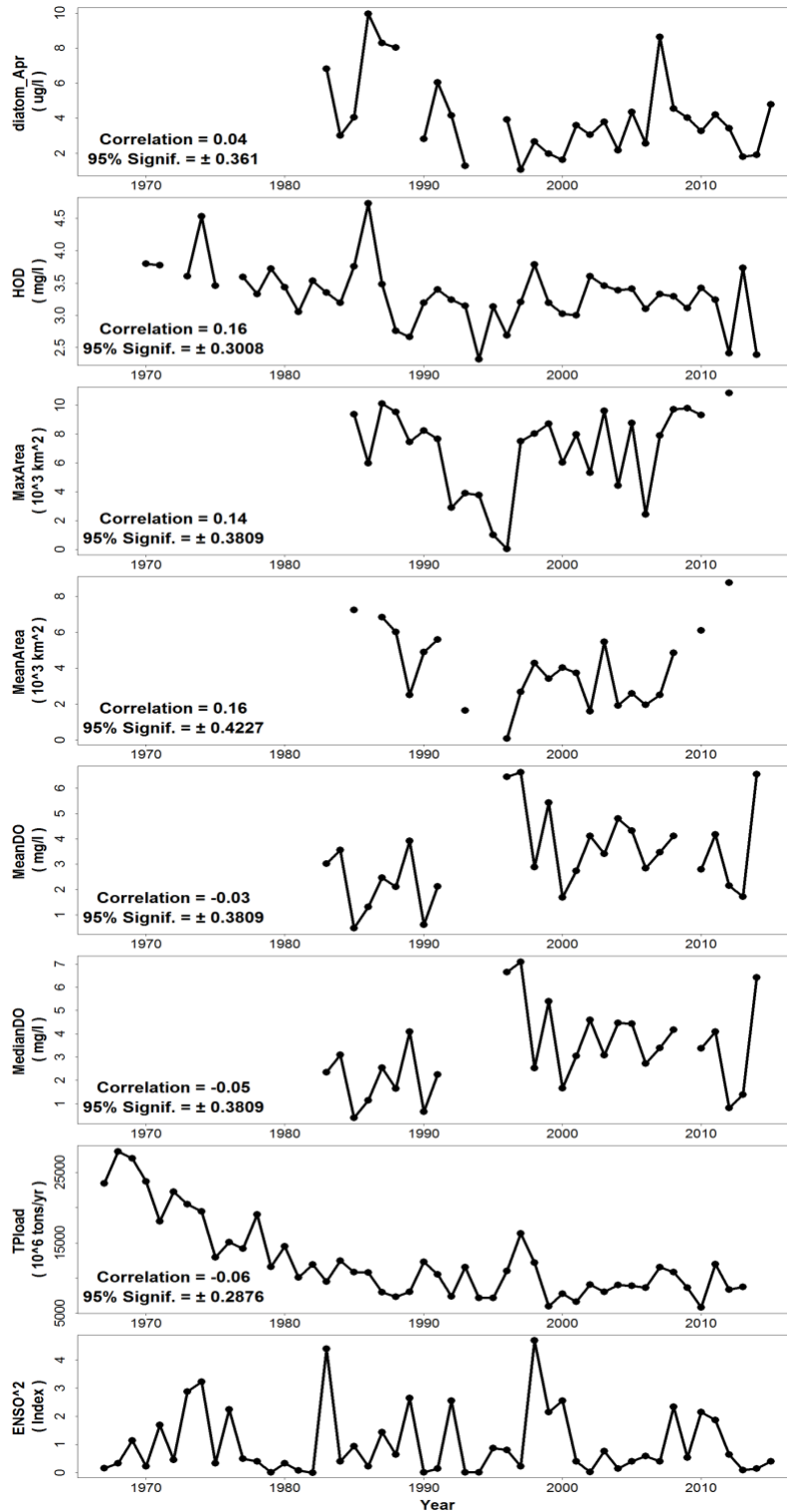


Figure 5. Correlation between ENSO² and biological parameters.

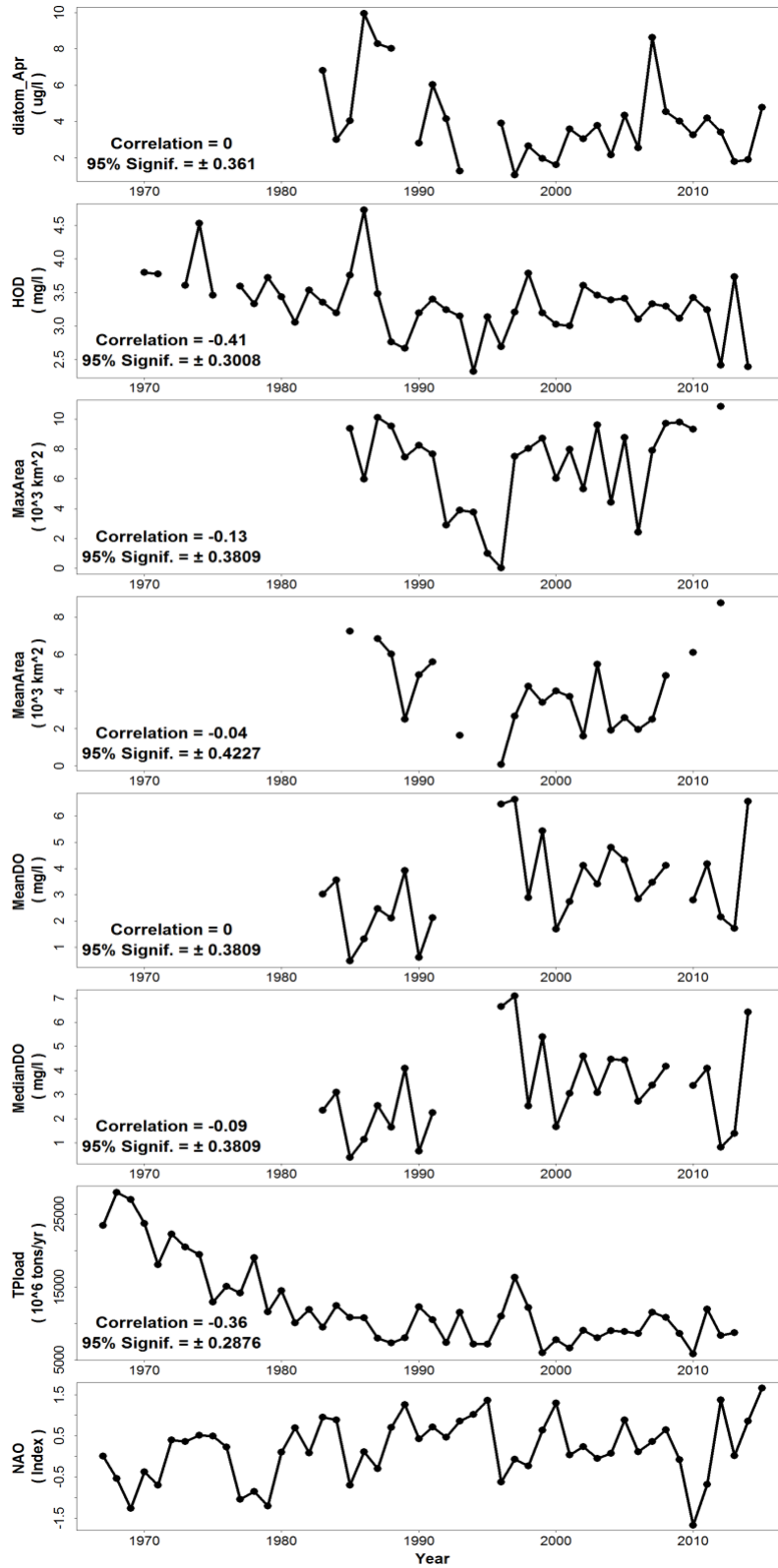


Figure 6. Correlation between NAO and biological parameters.

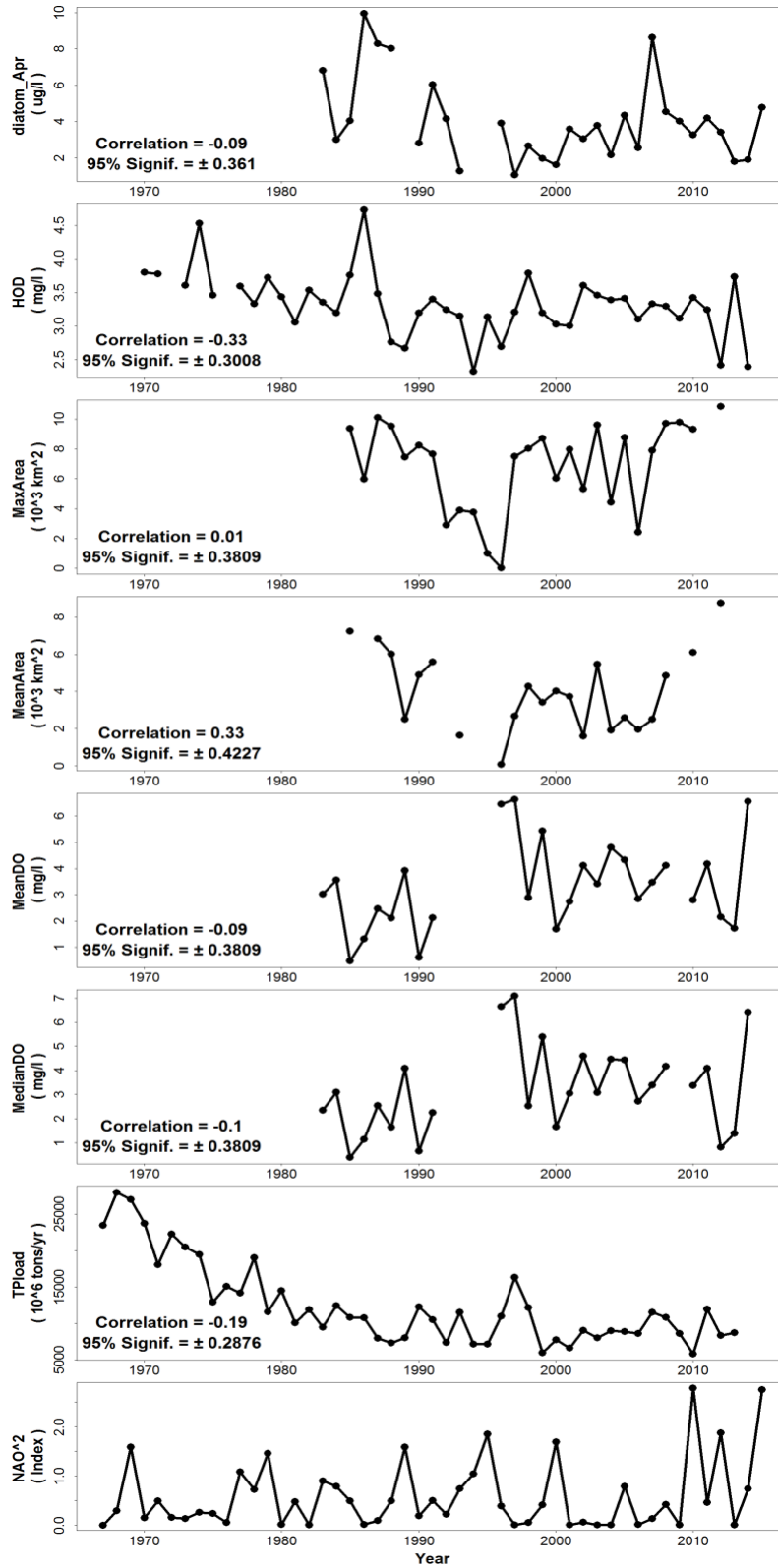


Figure 7. Correlation between NAO² and biological parameters.

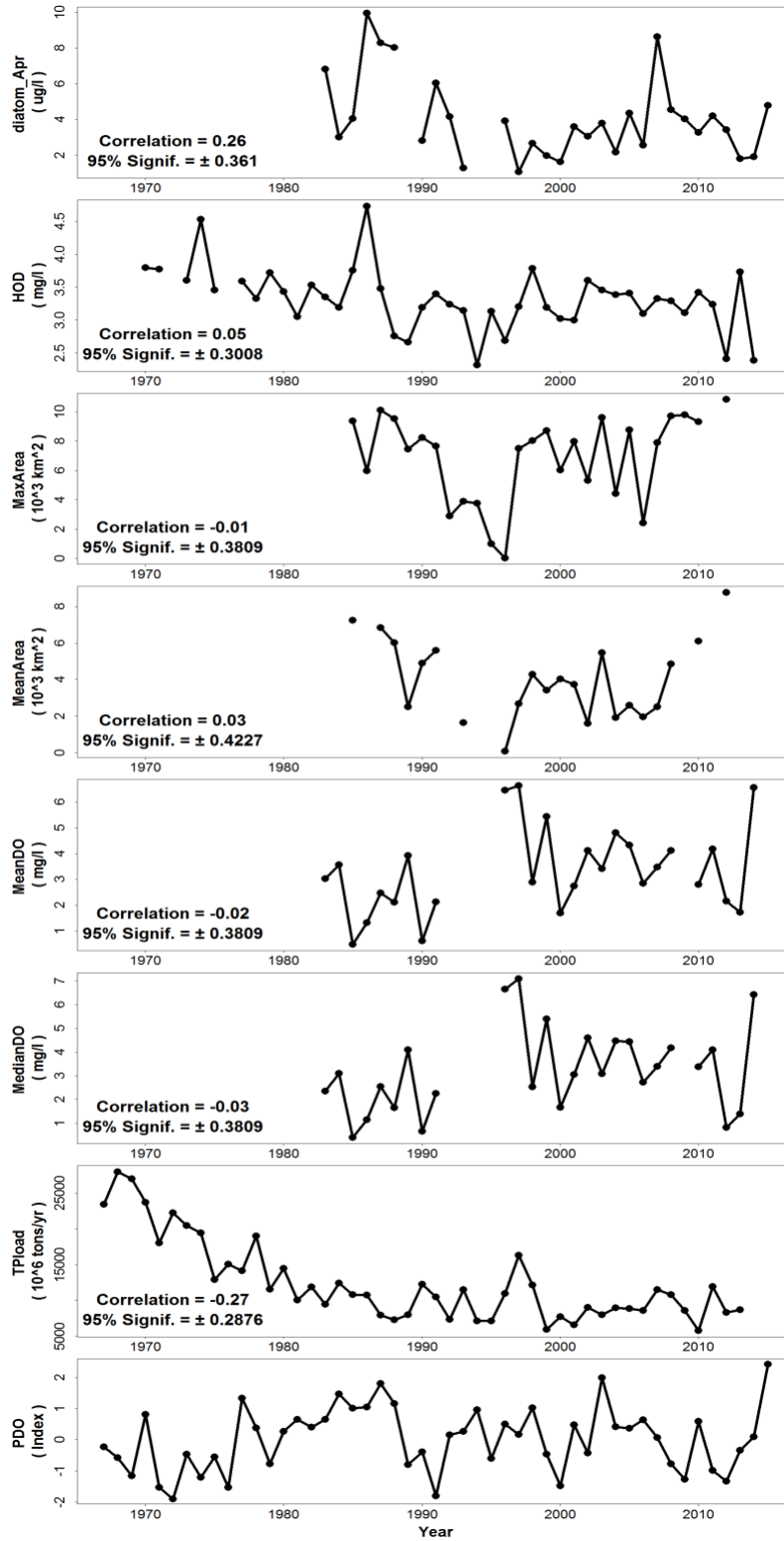


Figure 8. Correlation between PDO and biological parameters.

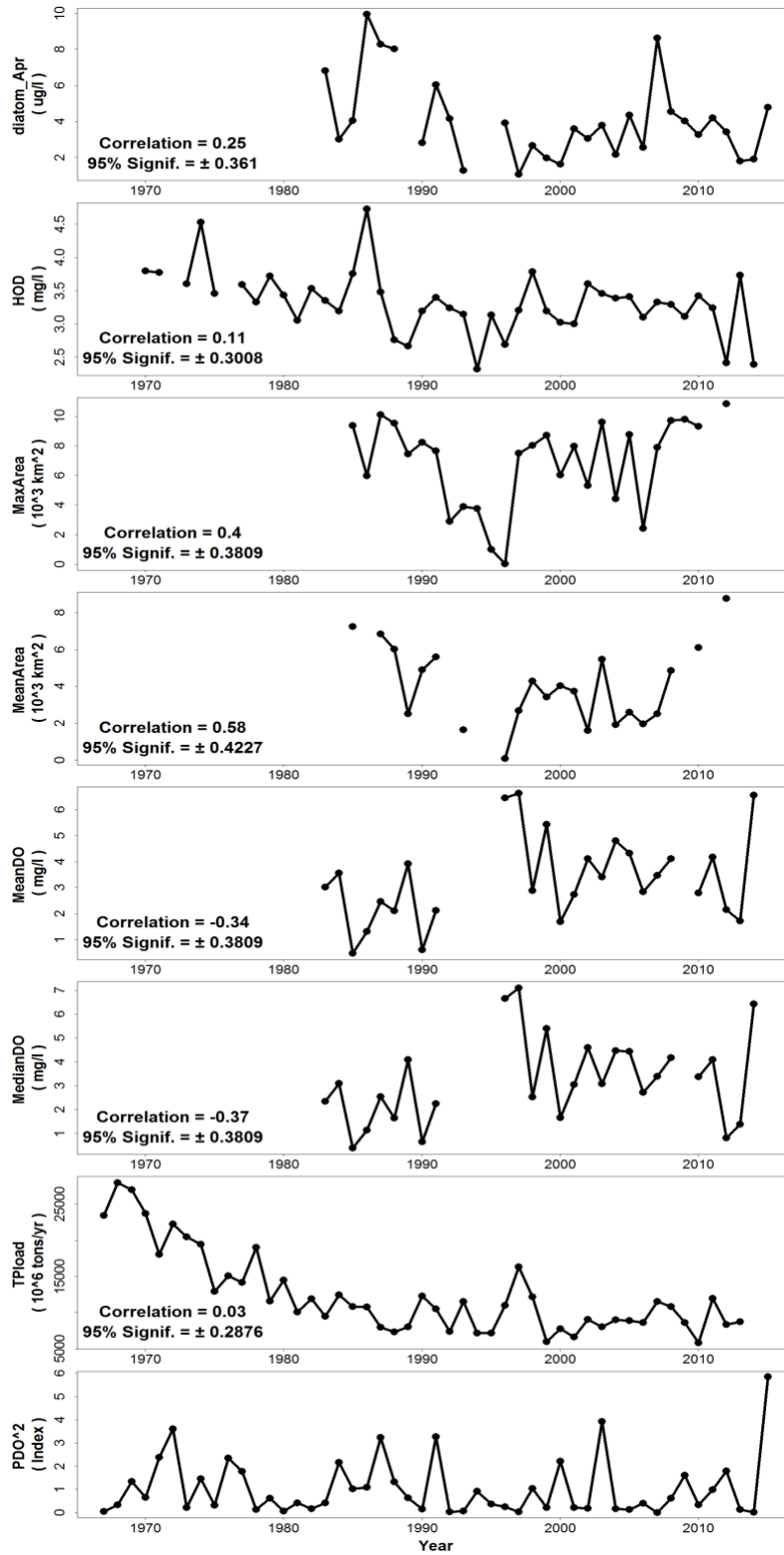


Figure 9. Correlation between PDO² and biological parameters.

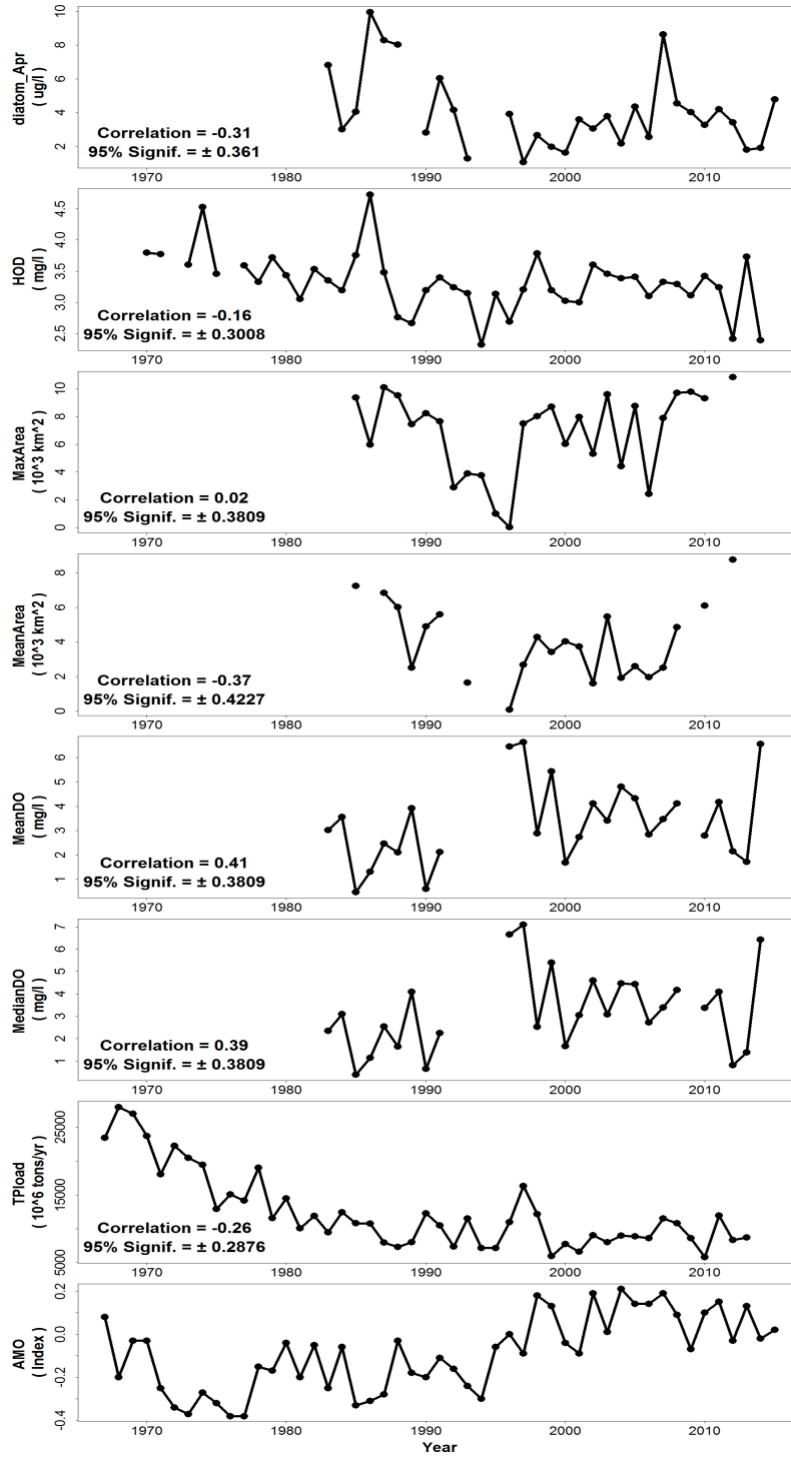


Figure 10. Linear correlation between AMO and biological parameters.

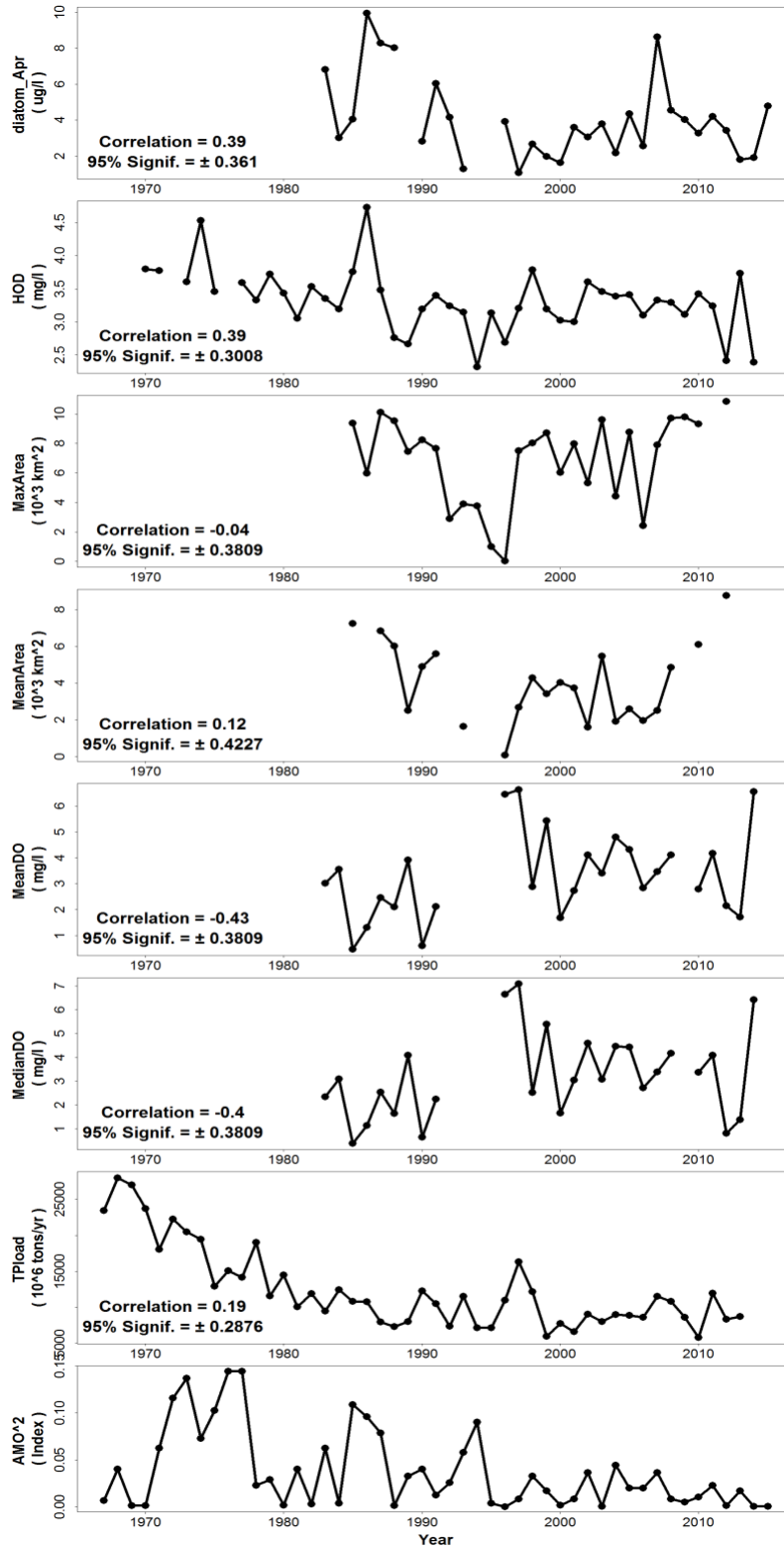


Figure 11. Correlation between AMO^2 (quadratic or nonlinear) and biological parameters.

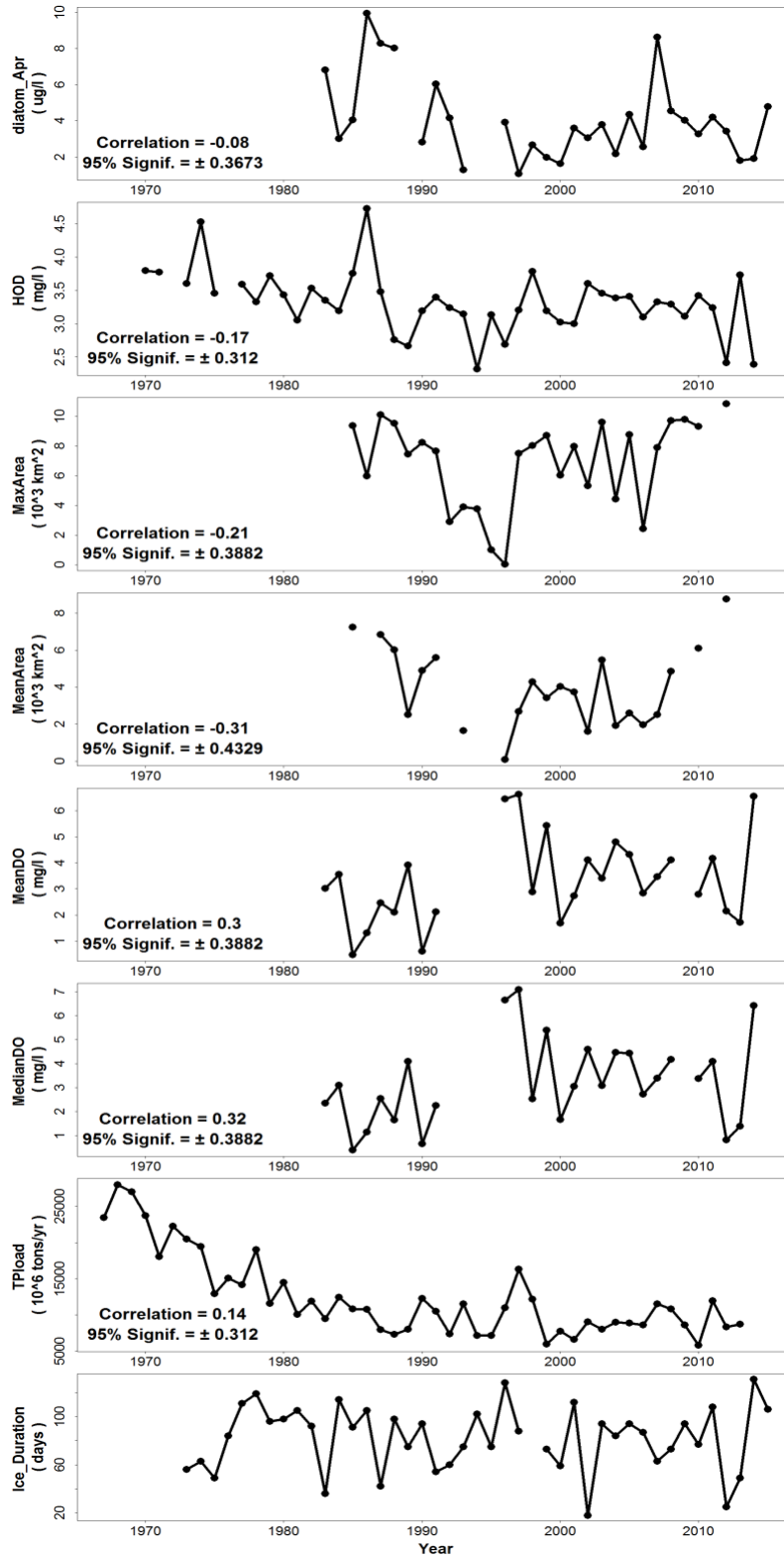


Figure 12. Correlation between ice duration and biological parameters.

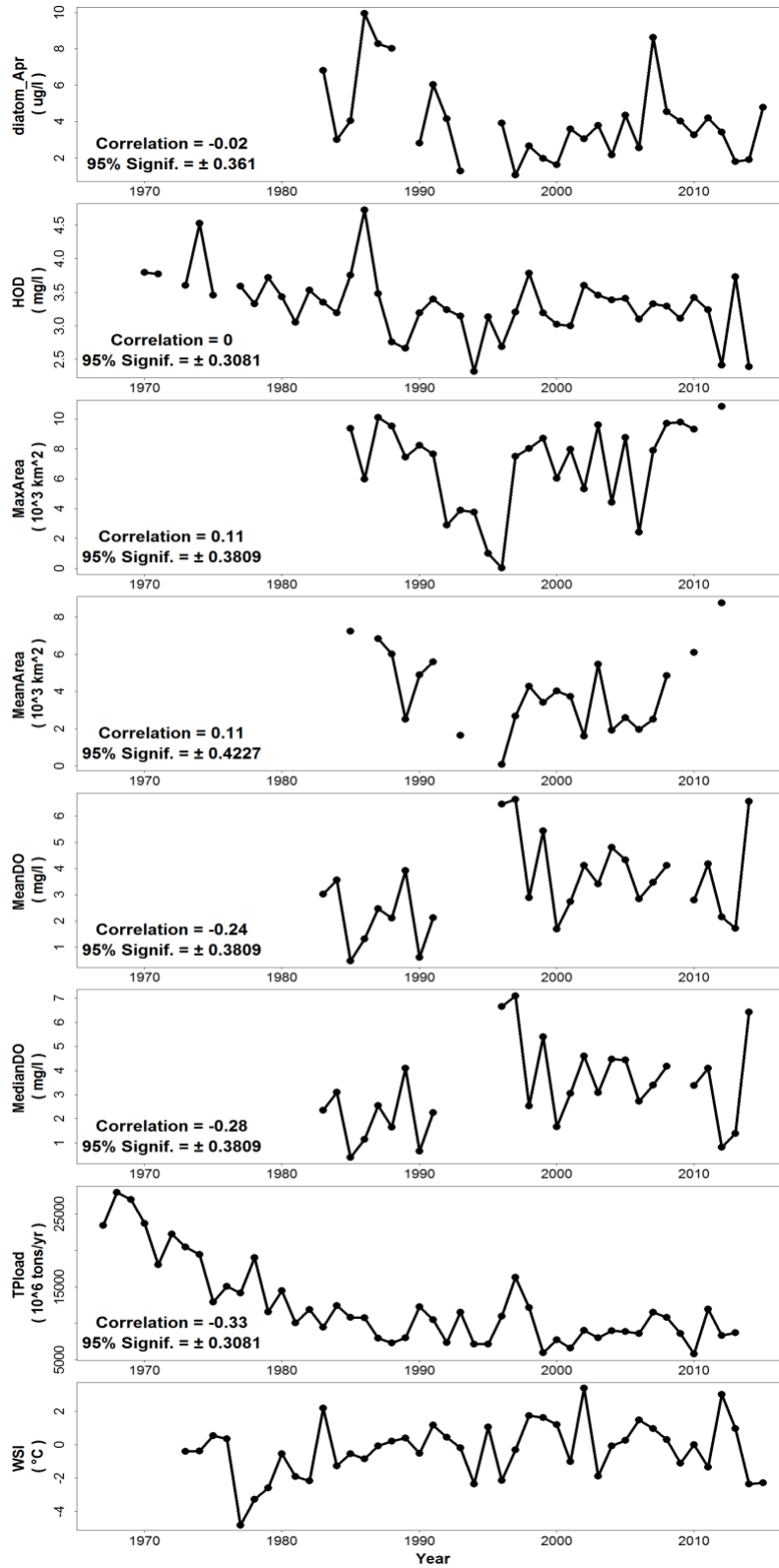


Figure 13. Correlation between WSI and biological parameters.

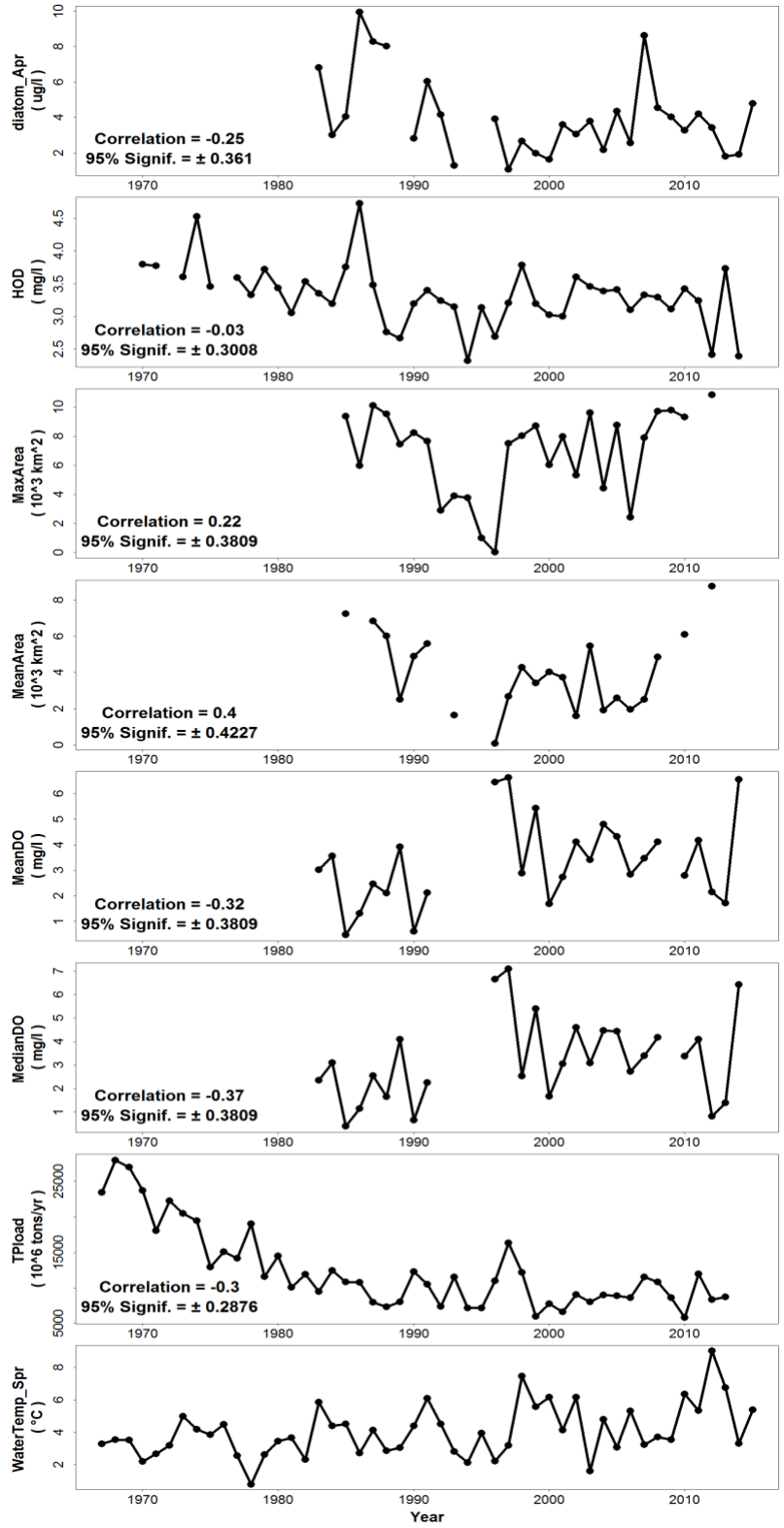


Figure 14. Correlation between spring water temperature and biological parameters.

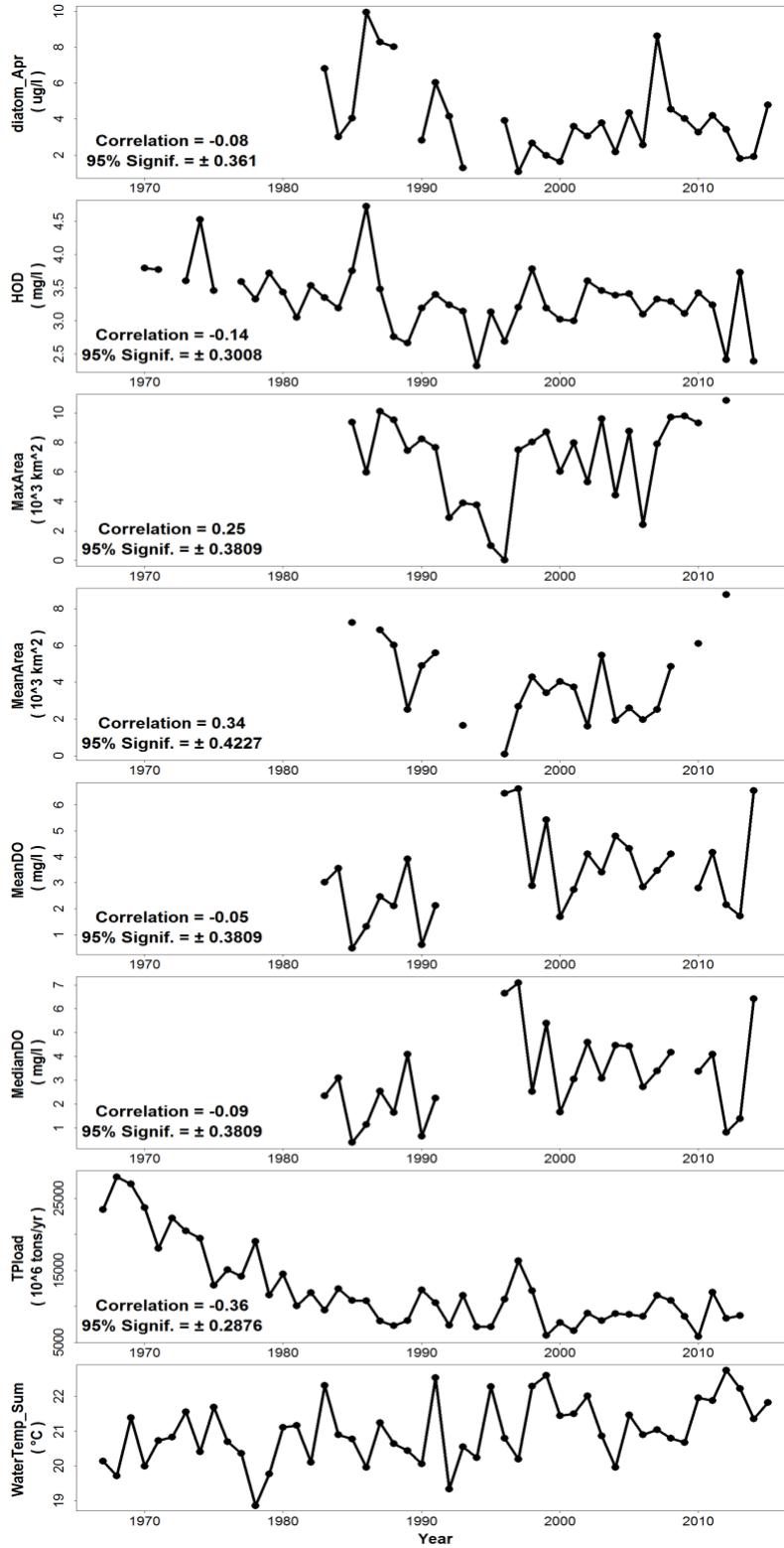


Figure 15. Correlation between summer water temperature and biological parameters.

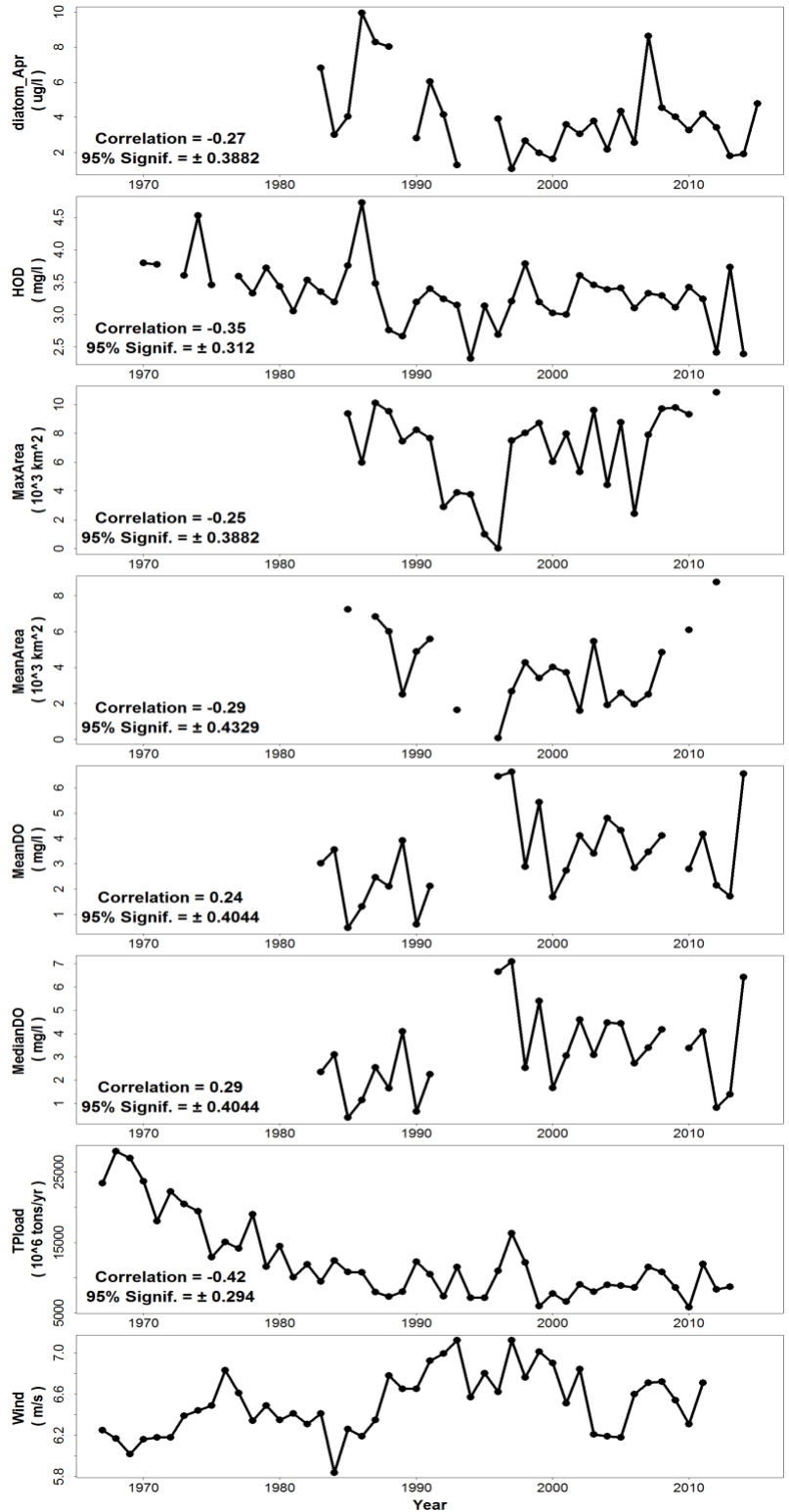


Figure 16. Correlation between wind speed and biological parameters.

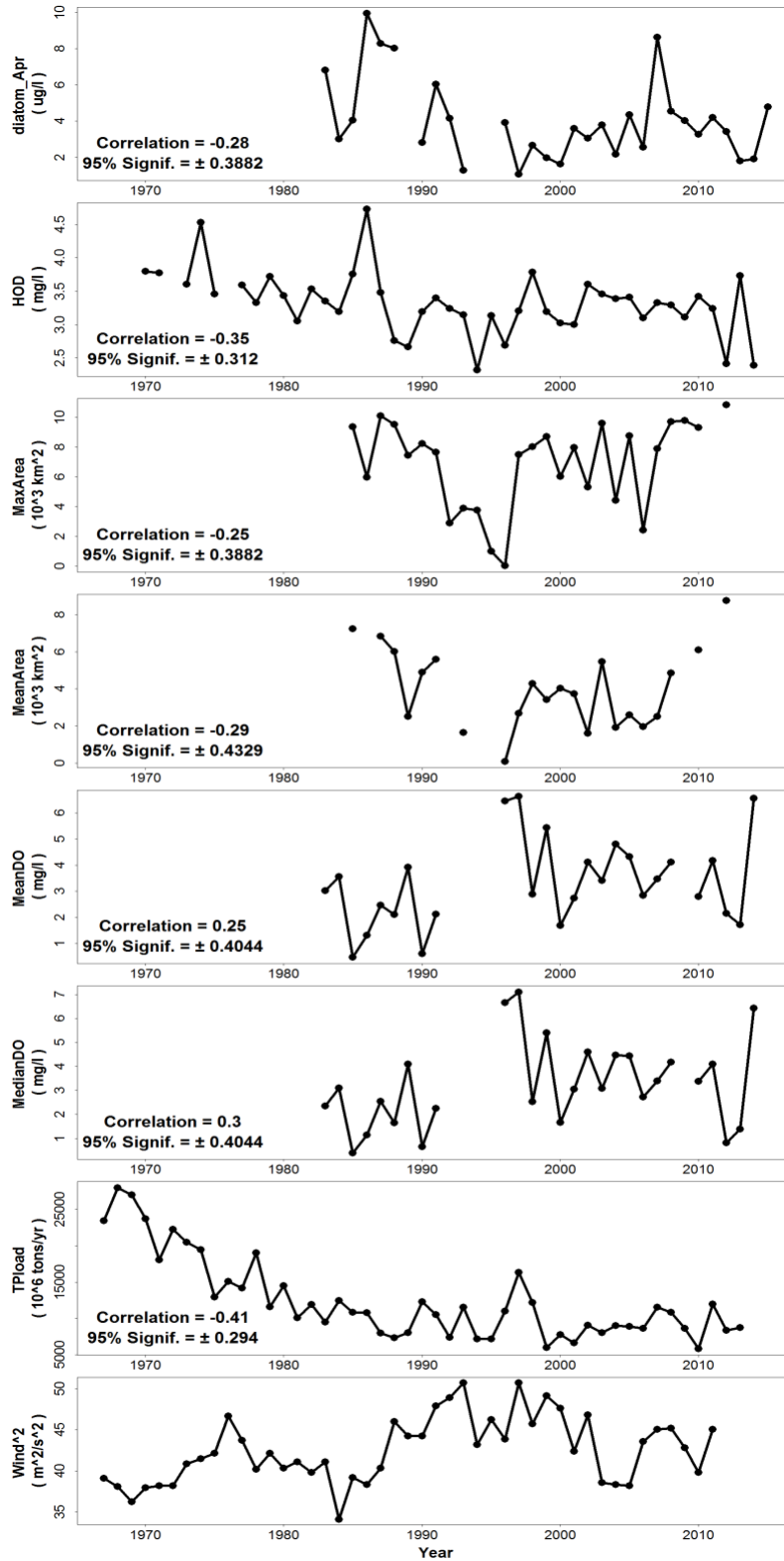


Figure 17. Correlation between wind speed squared (quadratic; equivalent to wind stress) and biological parameters.

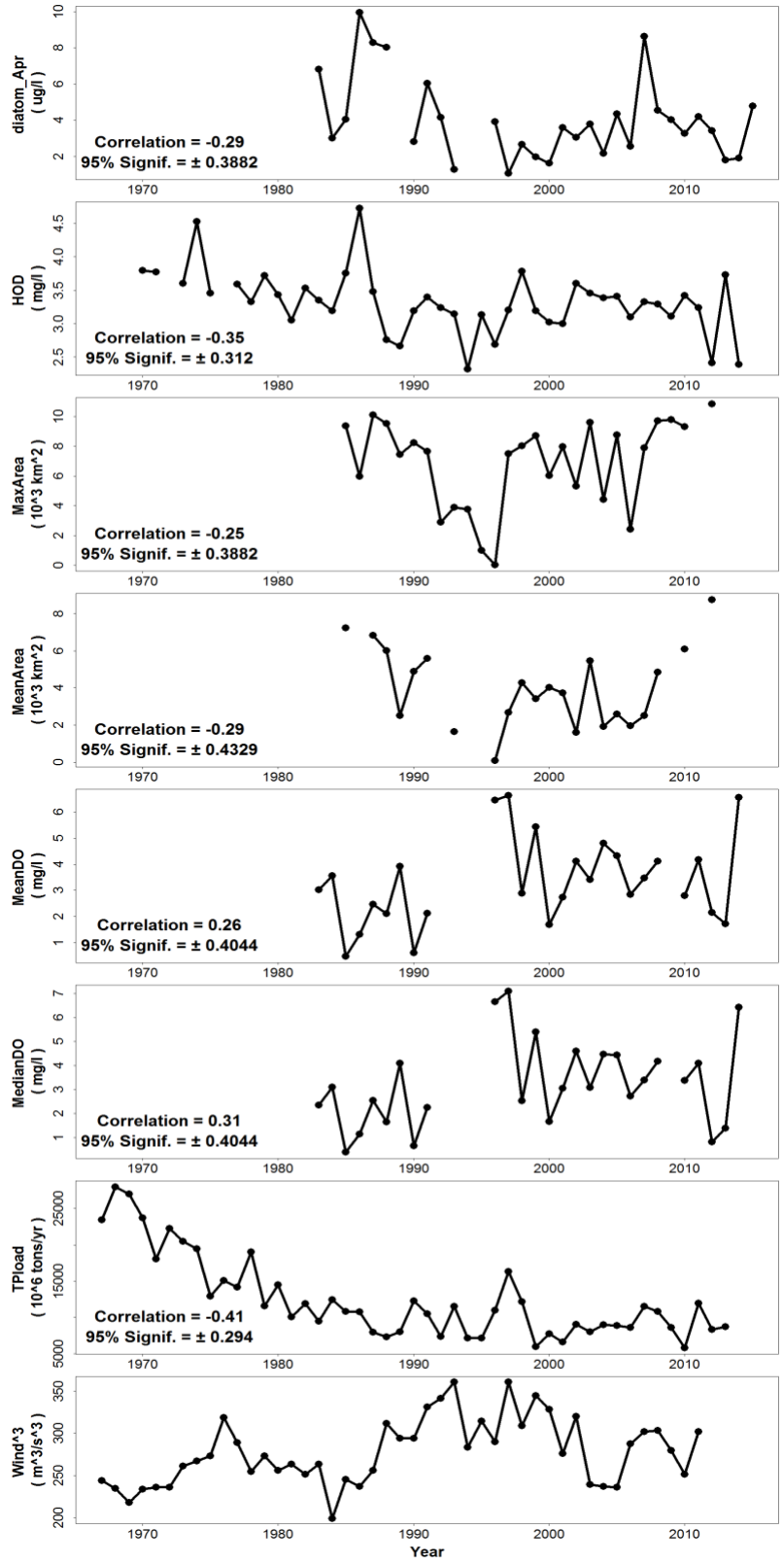


Figure 18. Correlation between wind speed cubed (equivalent to wind mixing) and biological parameters.

4.2 Linear regression between environmental forcings and biological parameters

This section examines the relationship between the physical/environmental forcings and biological parameters using scatter plots and linear regression methods. If a linear regression is obtained at the 95% significance level (i.e., p value <0.05), the linear regression equation plus its root mean squared error or regression standard error is presented; otherwise, a quadratic (non-linear) curve is fit to the data. If the quadratic fit is close to the insignificant linear regression line, the non-linear relationship is not significant. The 95% critical values for Pearson's correlation coefficient are given.

The purpose of the scatter plots with a linear regression equation is to provide users the first glimpse of the relationship between the pair: linear or non-linear. To estimate the combined impacts of physical forcings, a comprehensive multi-variable regression model (equation) has to be used, such as in Wang et al. (2018), for the next step.

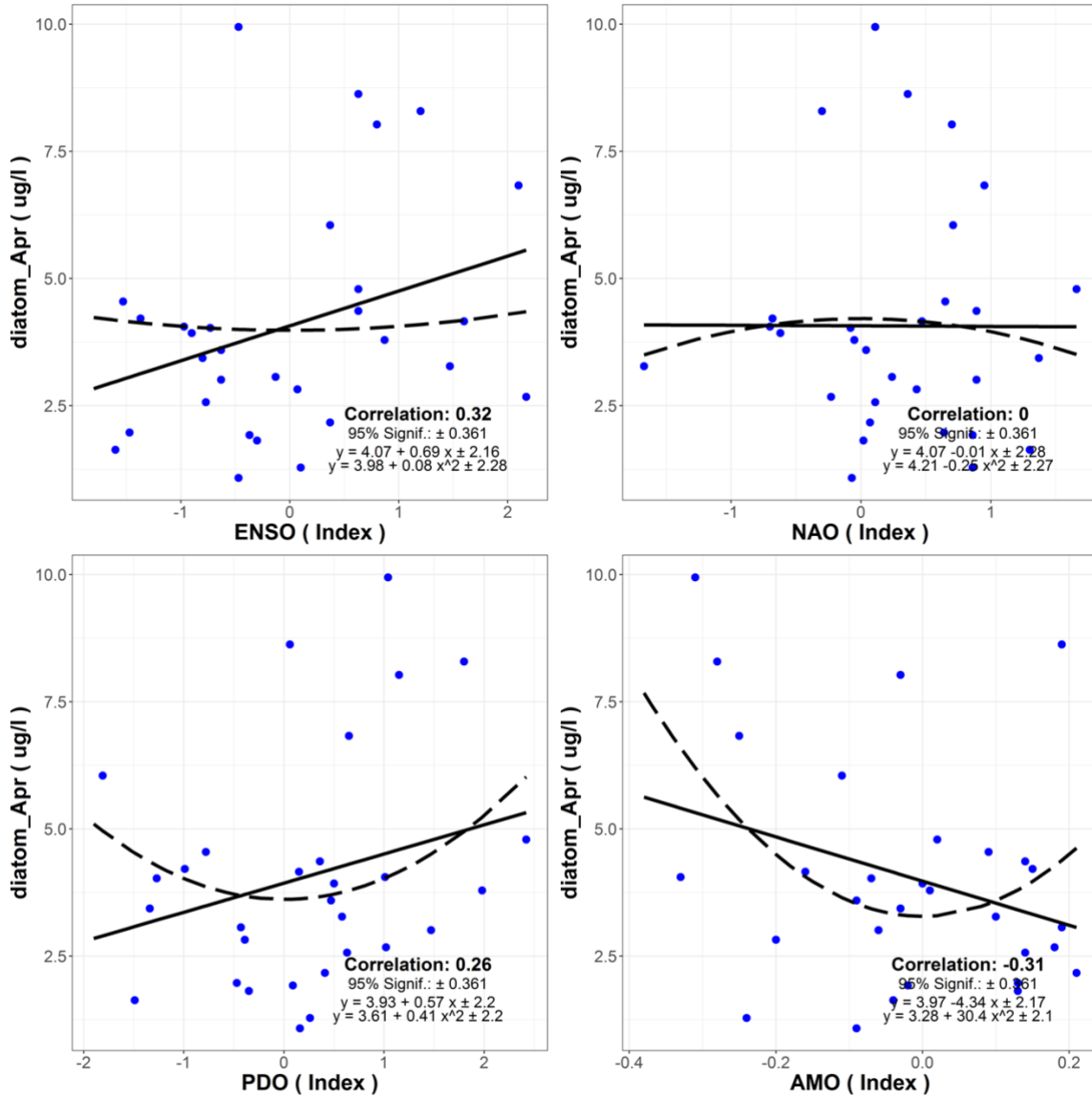


Figure 19. Regression between diatom in April and four atmospheric teleconnection patterns.

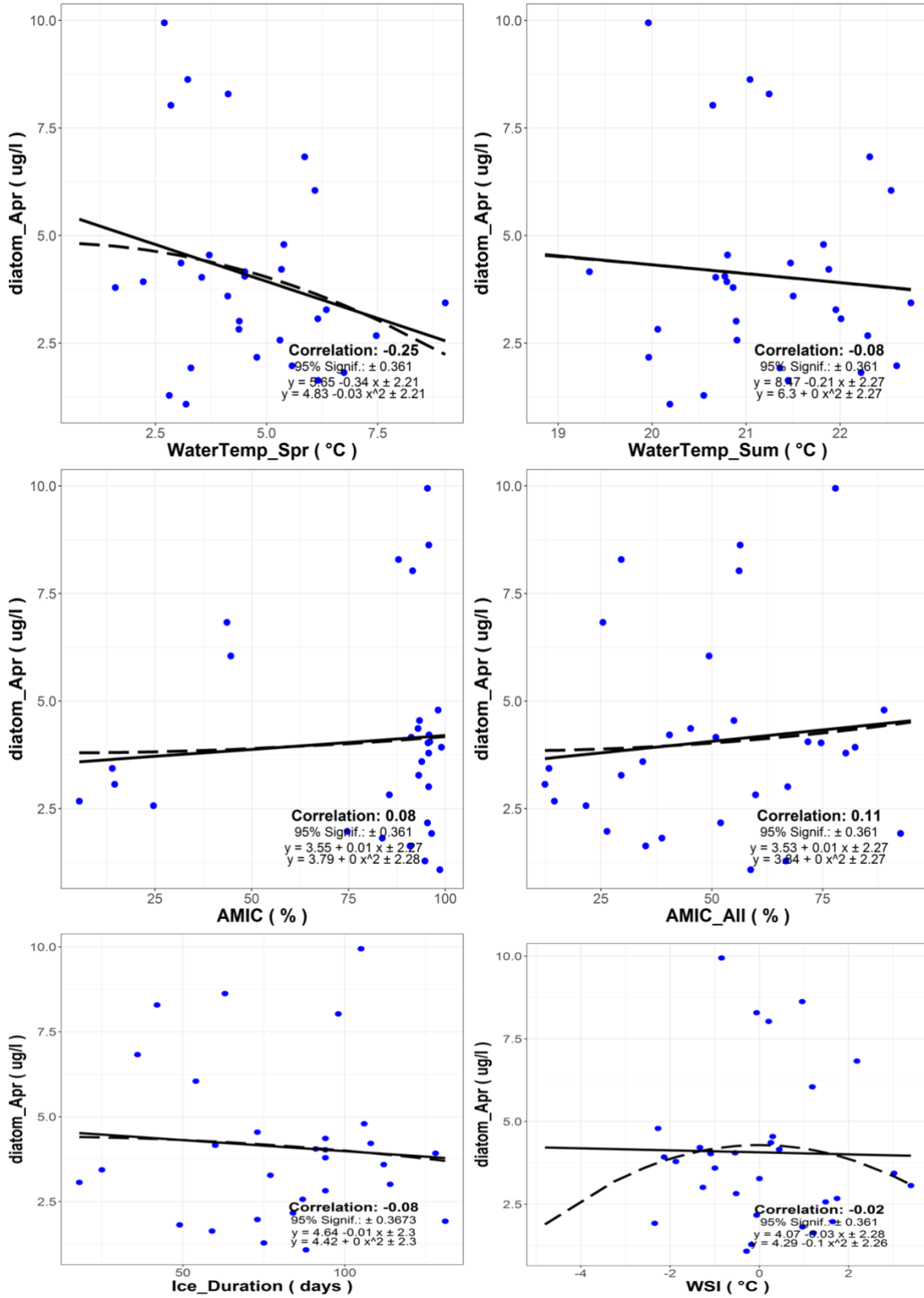


Figure 20. Regression between diatom in April and other physical forcings.

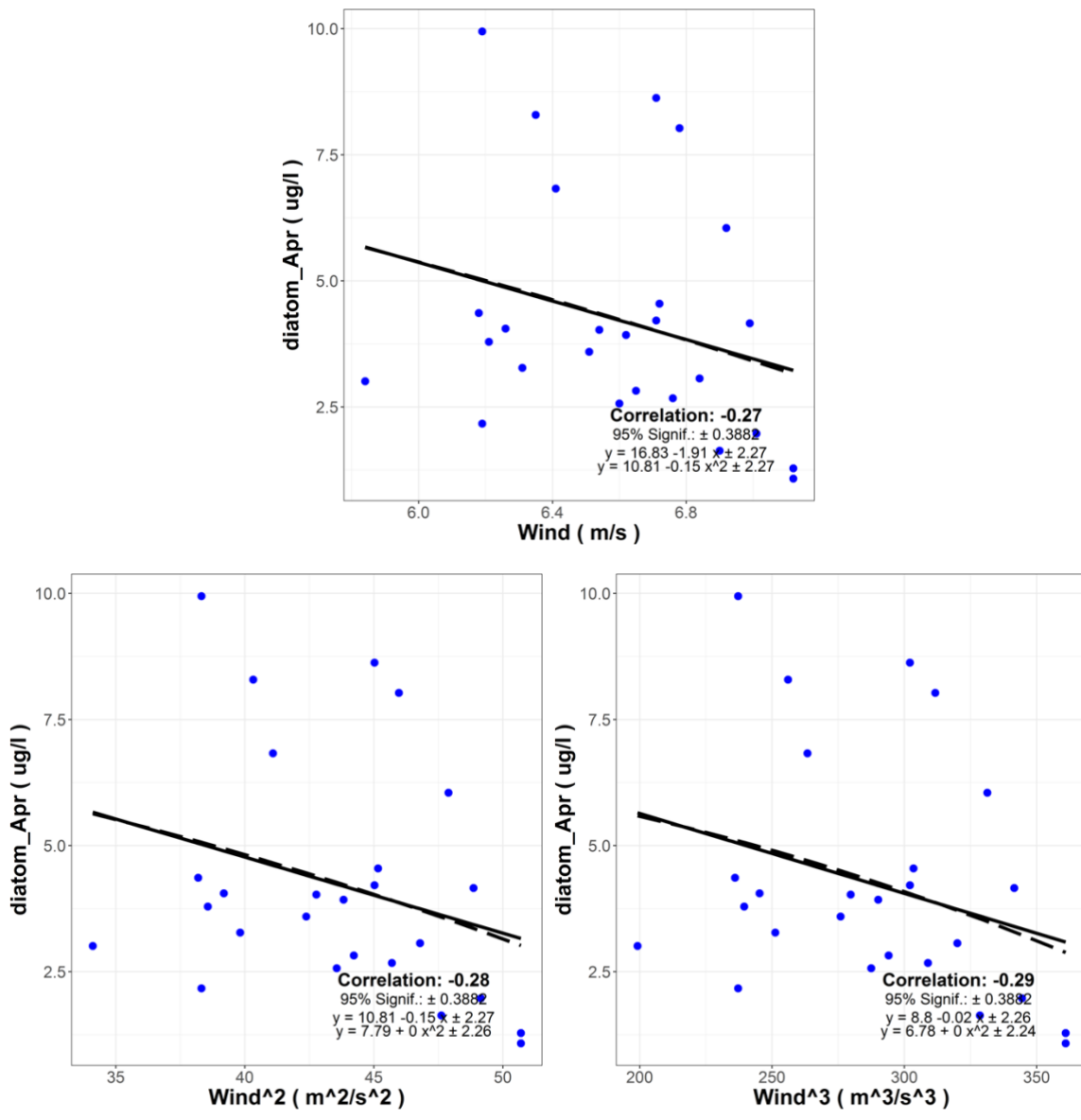


Figure 21. Regression between diatom in April and wind speed, its quadratic and cubed forms.

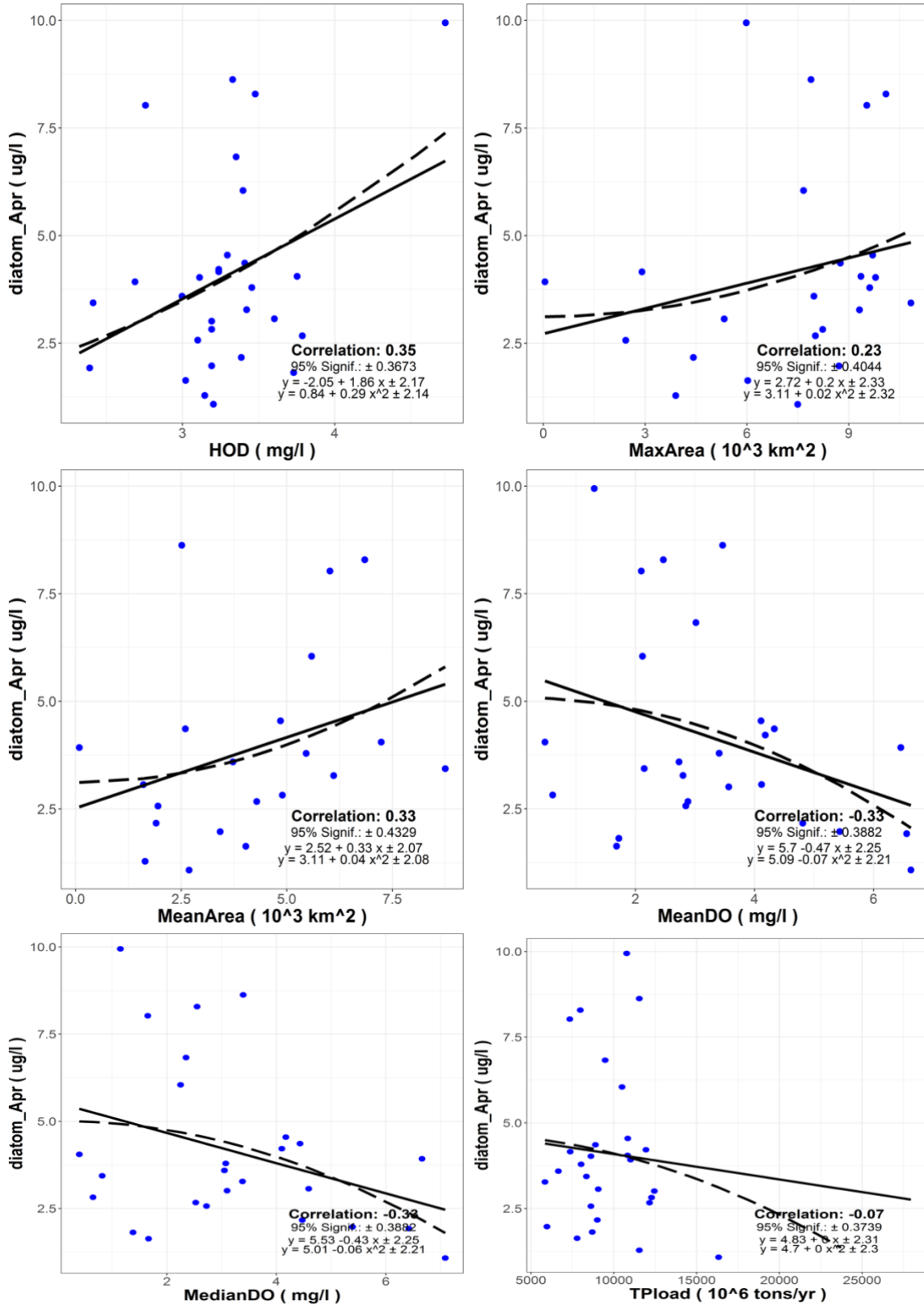


Figure 22. Regression between diatom in April and other biological parameters.

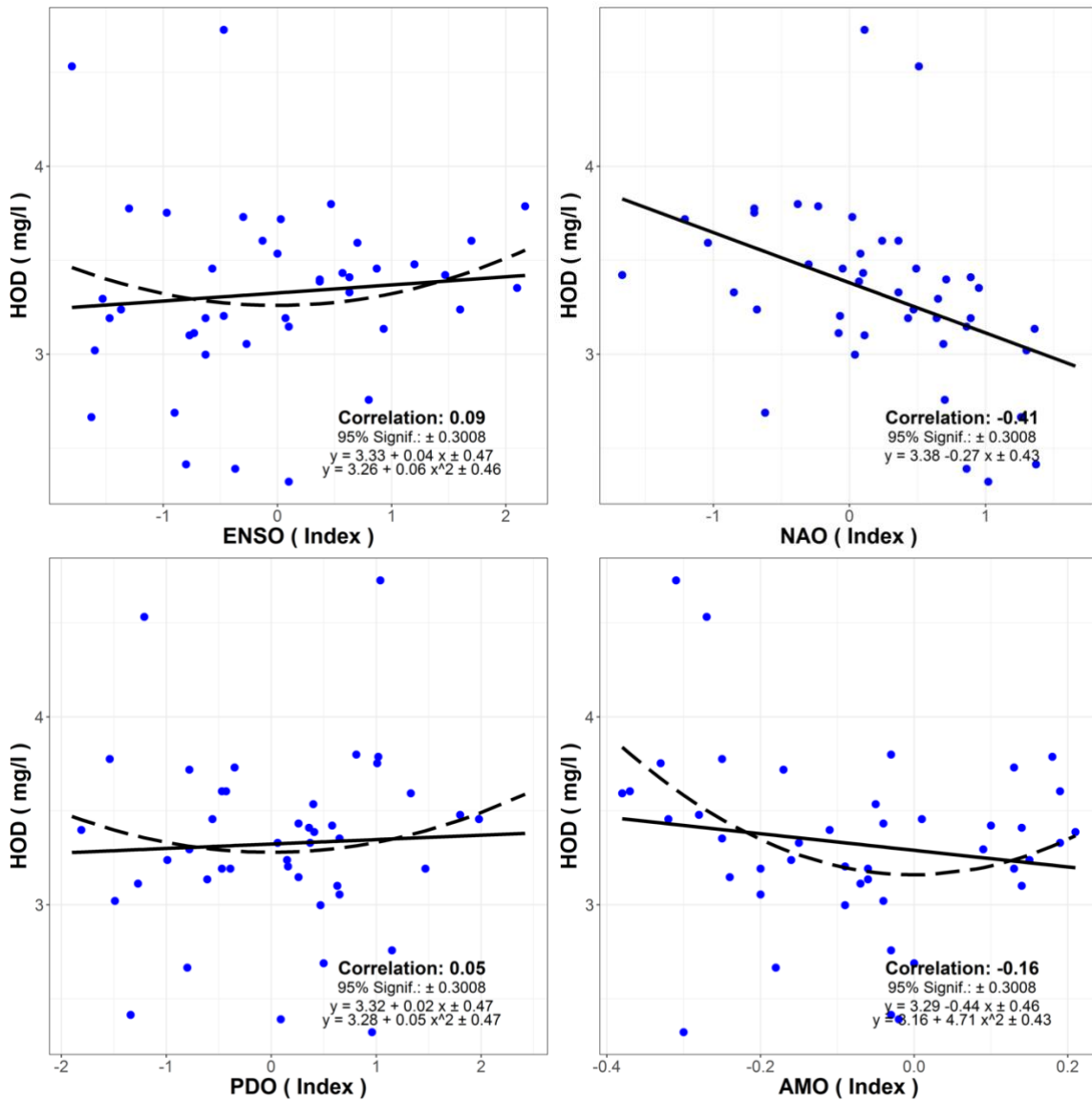


Figure 23. Regression between HOD and four teleconnection patterns.

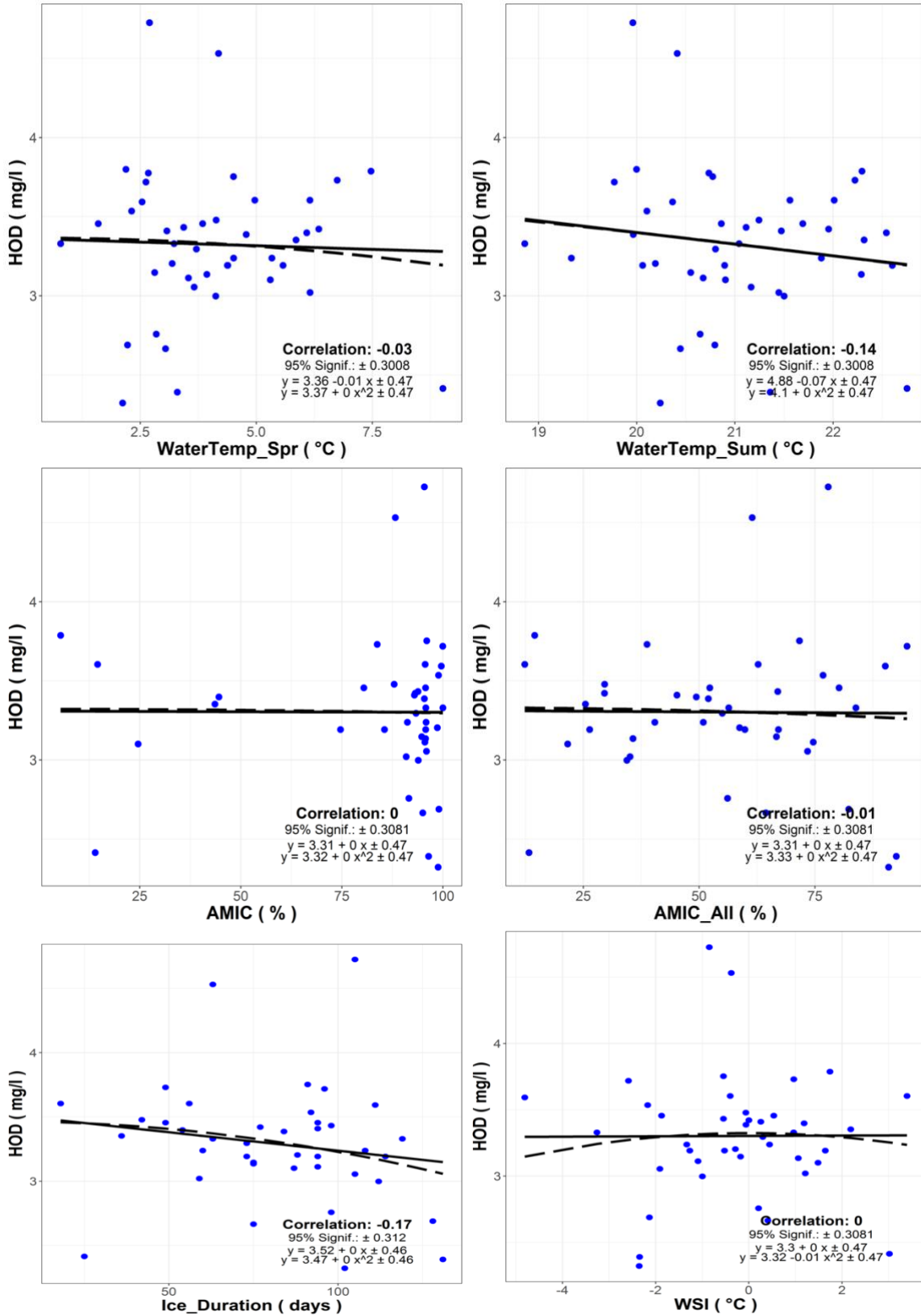


Figure 24. Regression between HOD and other physical forcings.

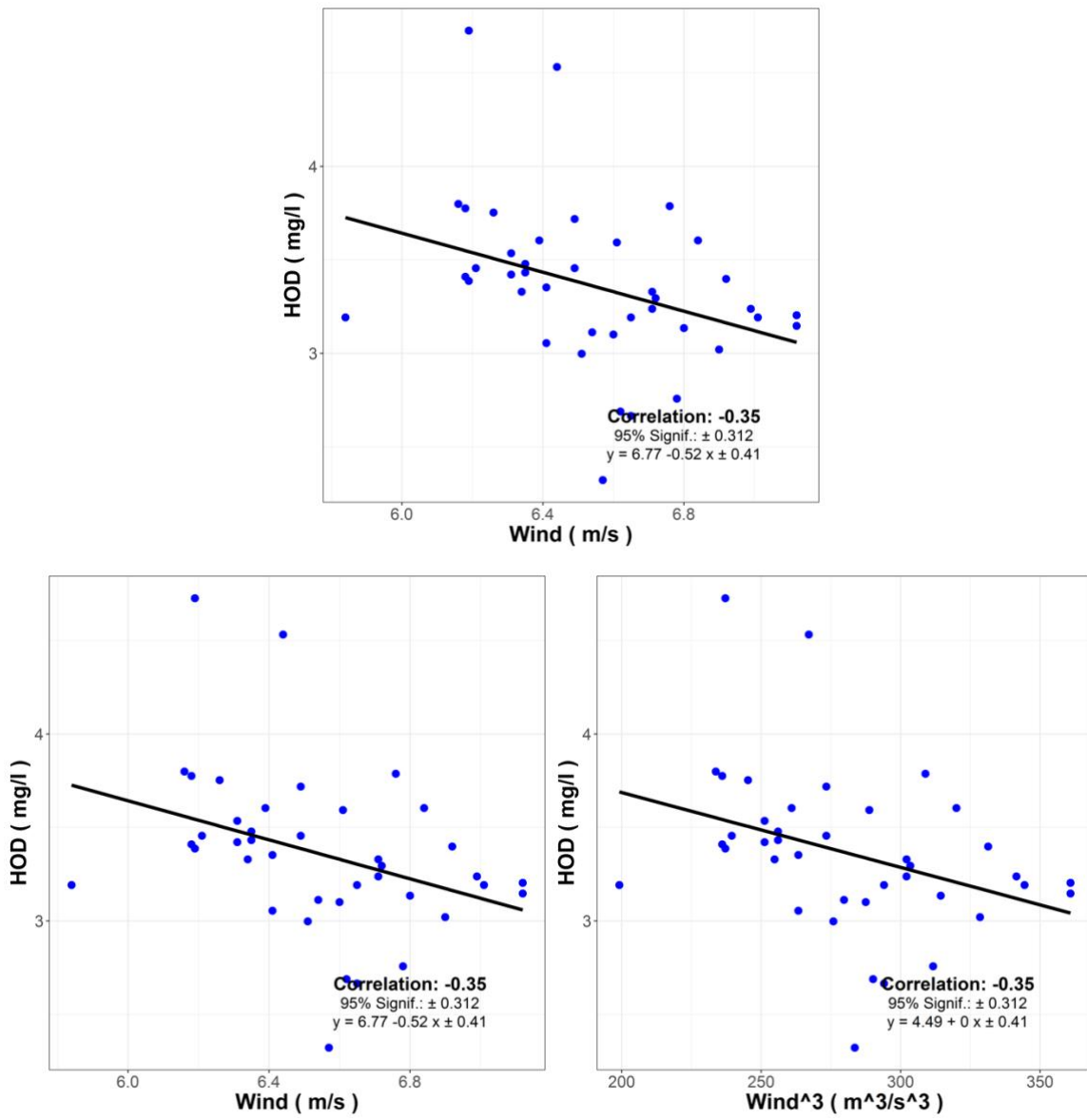


Figure 25. Regression between HOD and wind speed, its quadratic and cubed forms.

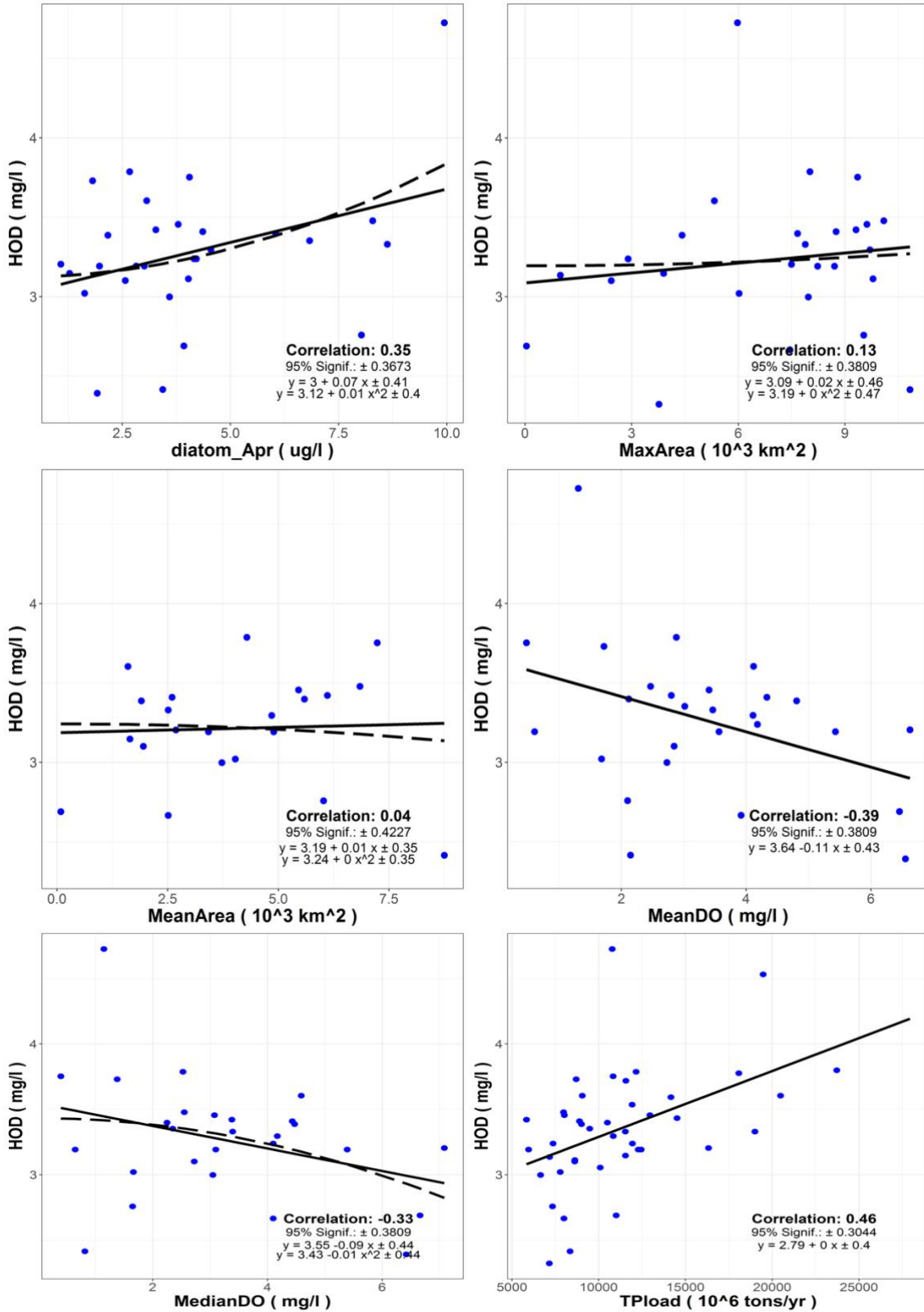


Figure 26. Regression between HOD and other biological parameters.

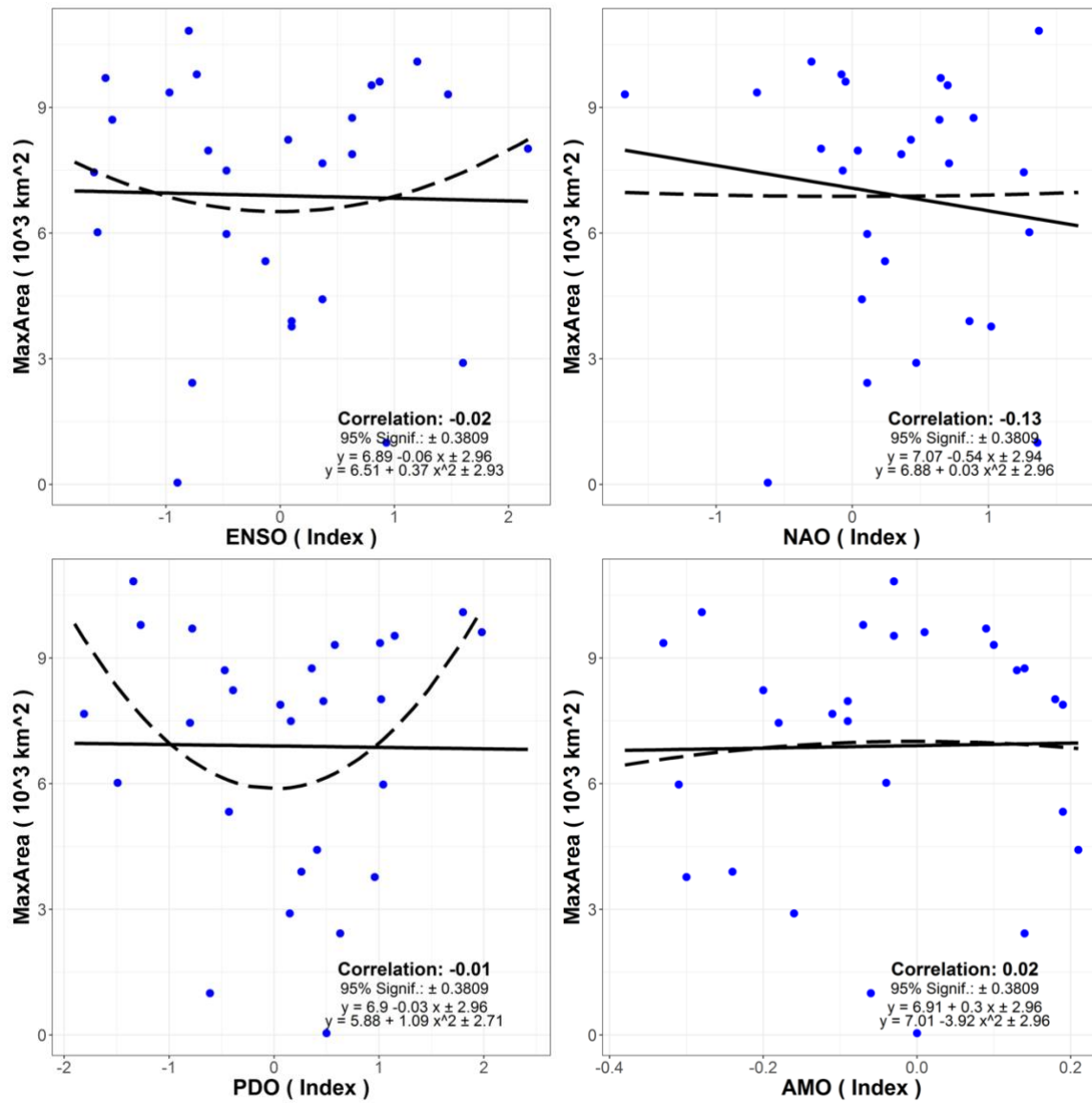


Figure 27. Regression between maximum hypoxia area and four teleconnection patterns.

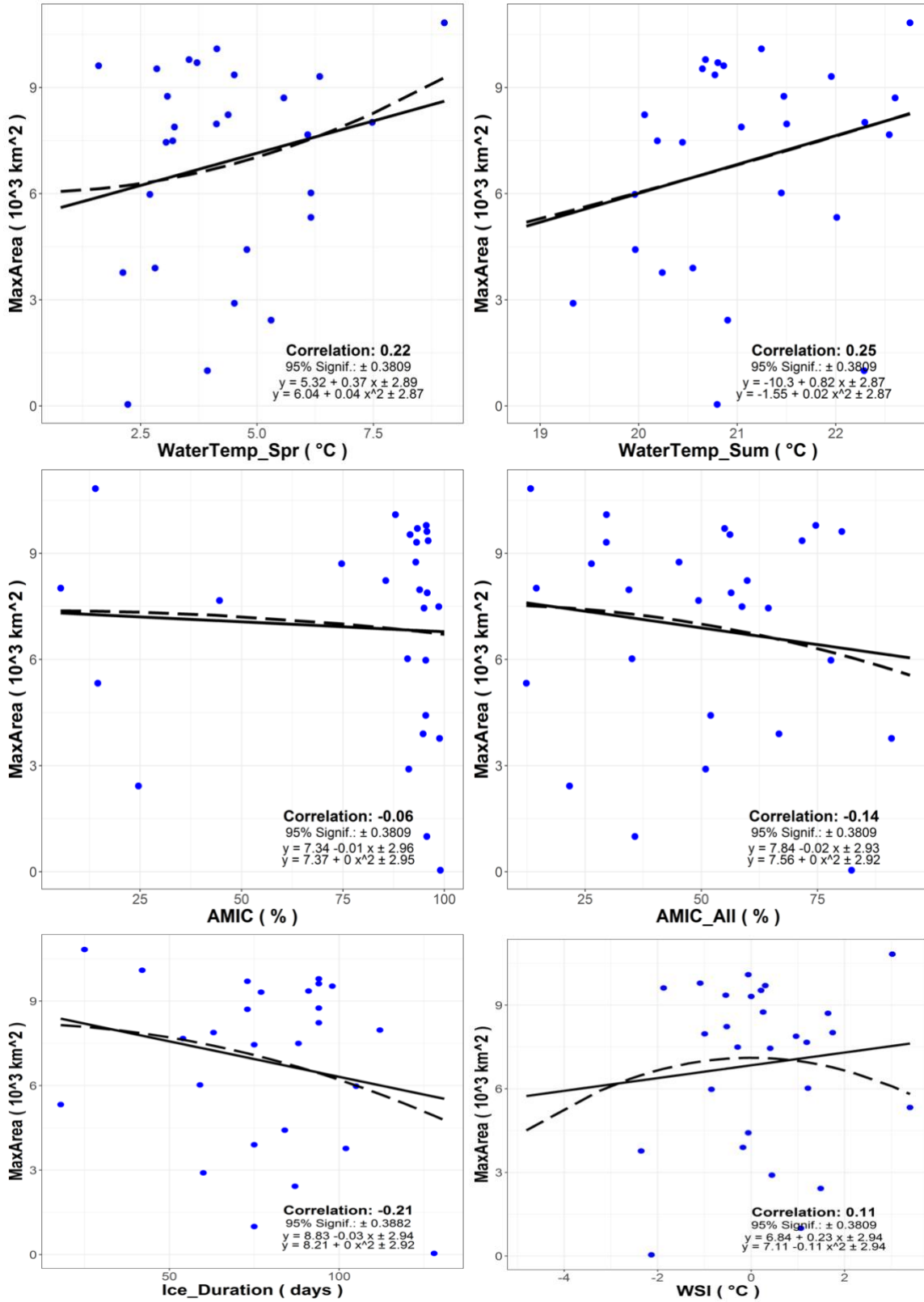


Figure 28. Regression between maximum hypoxia area and other physical forcings.

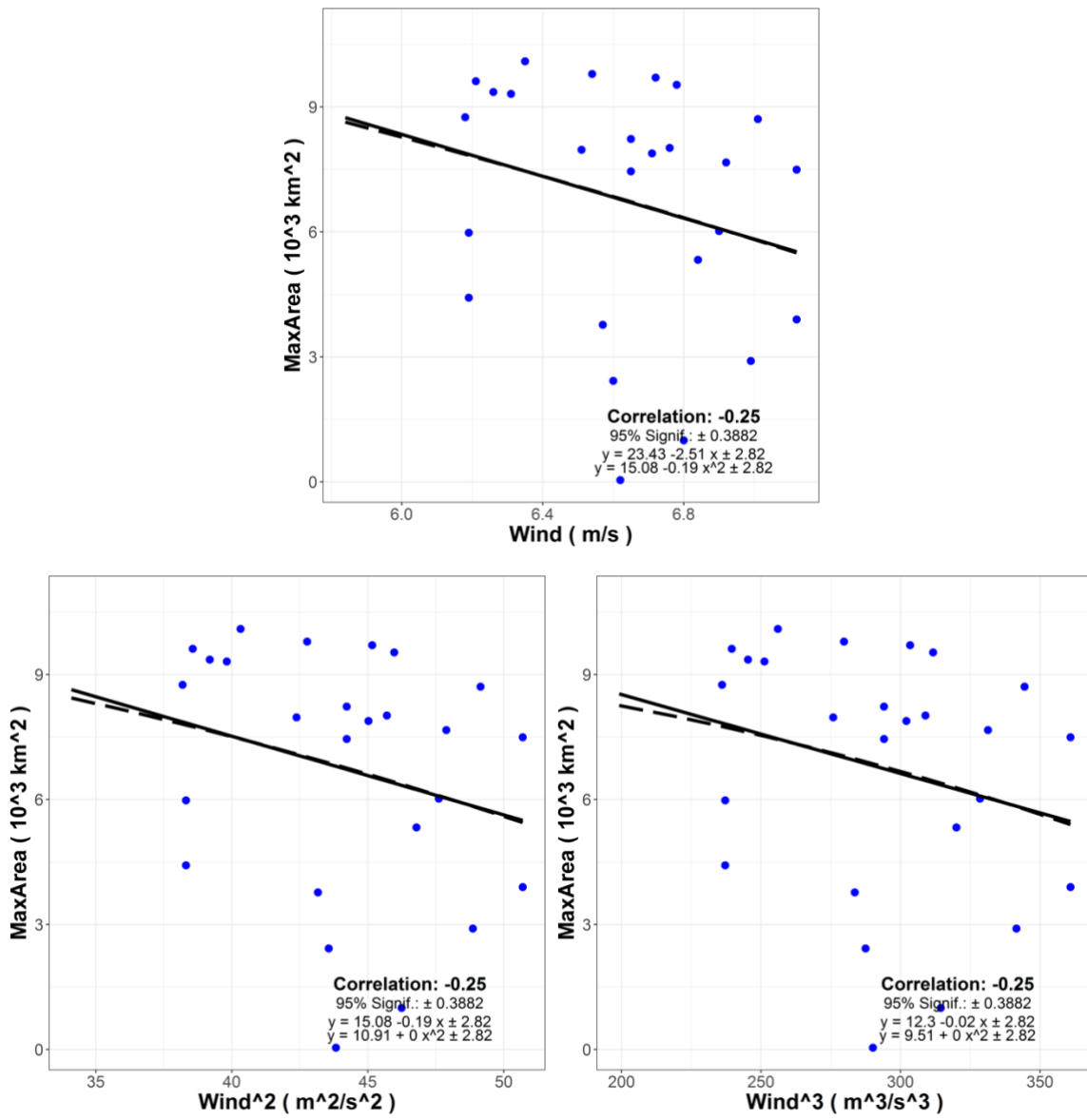


Figure 29. Regression between maximum hypoxia area and wind speed, its quadratic and cubed forms.

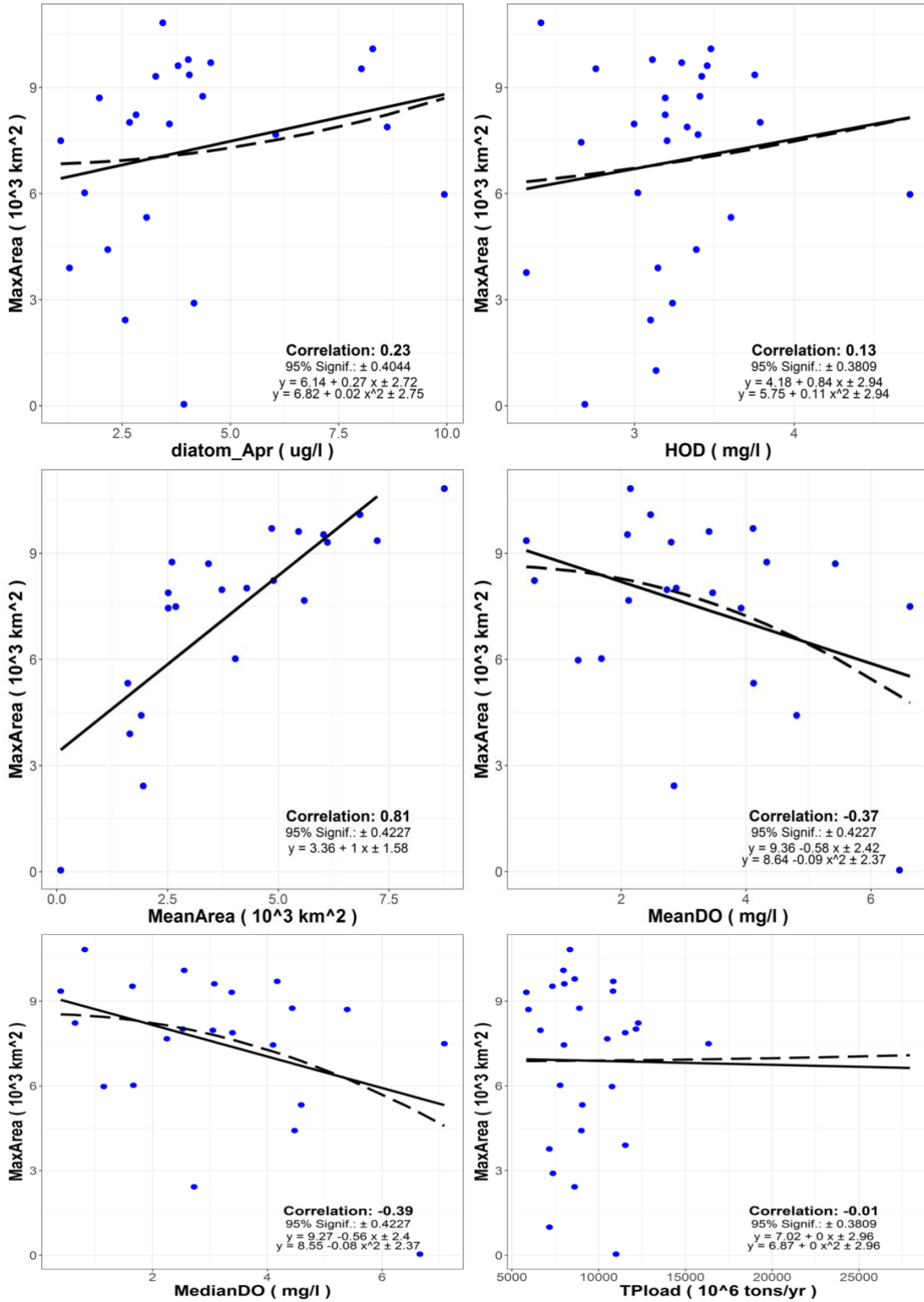


Figure 30. Regression between maximum hypoxia area and other biological parameters.

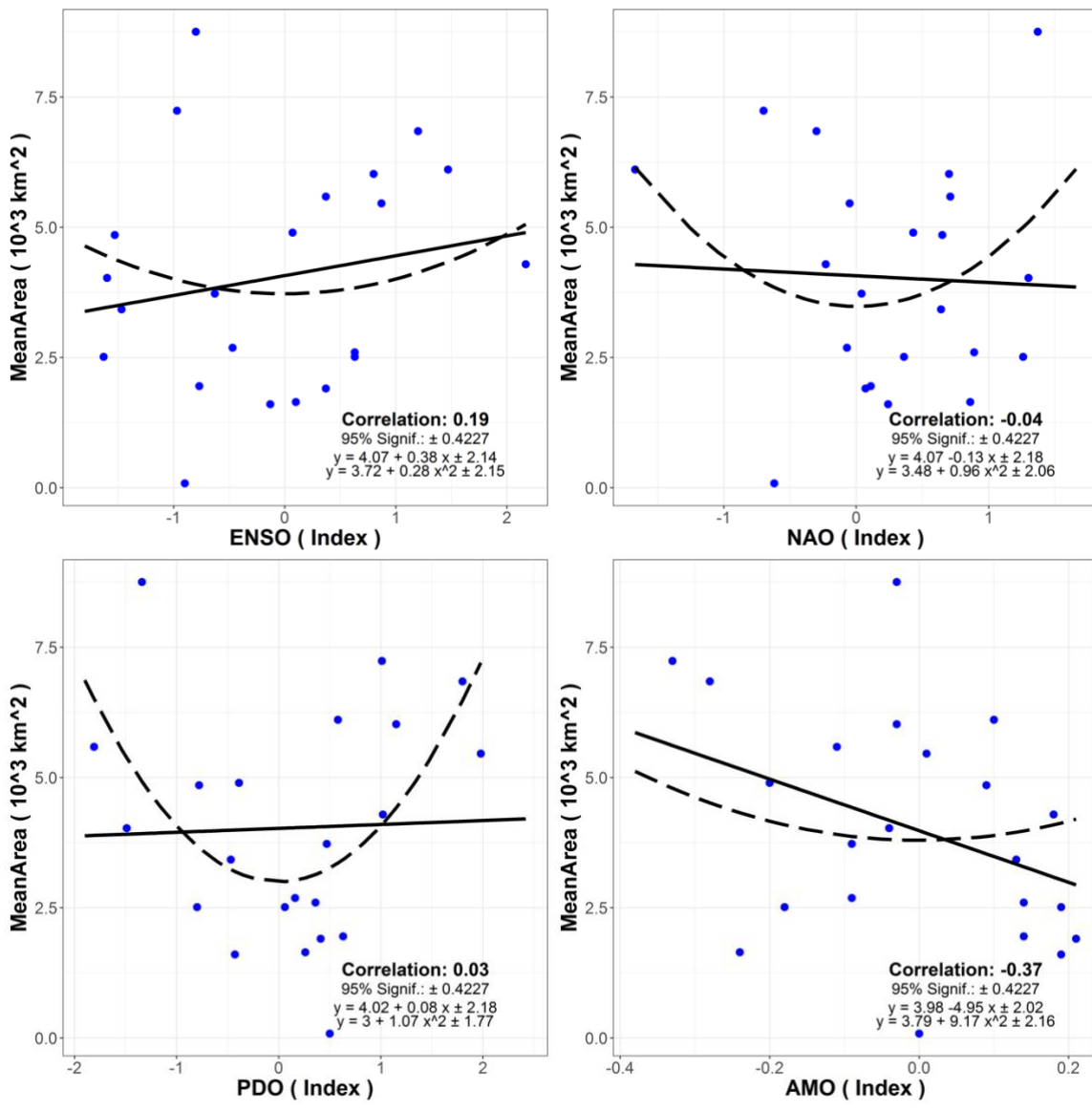


Figure 31. Regression between mean hypoxia area and four teleconnection patterns.

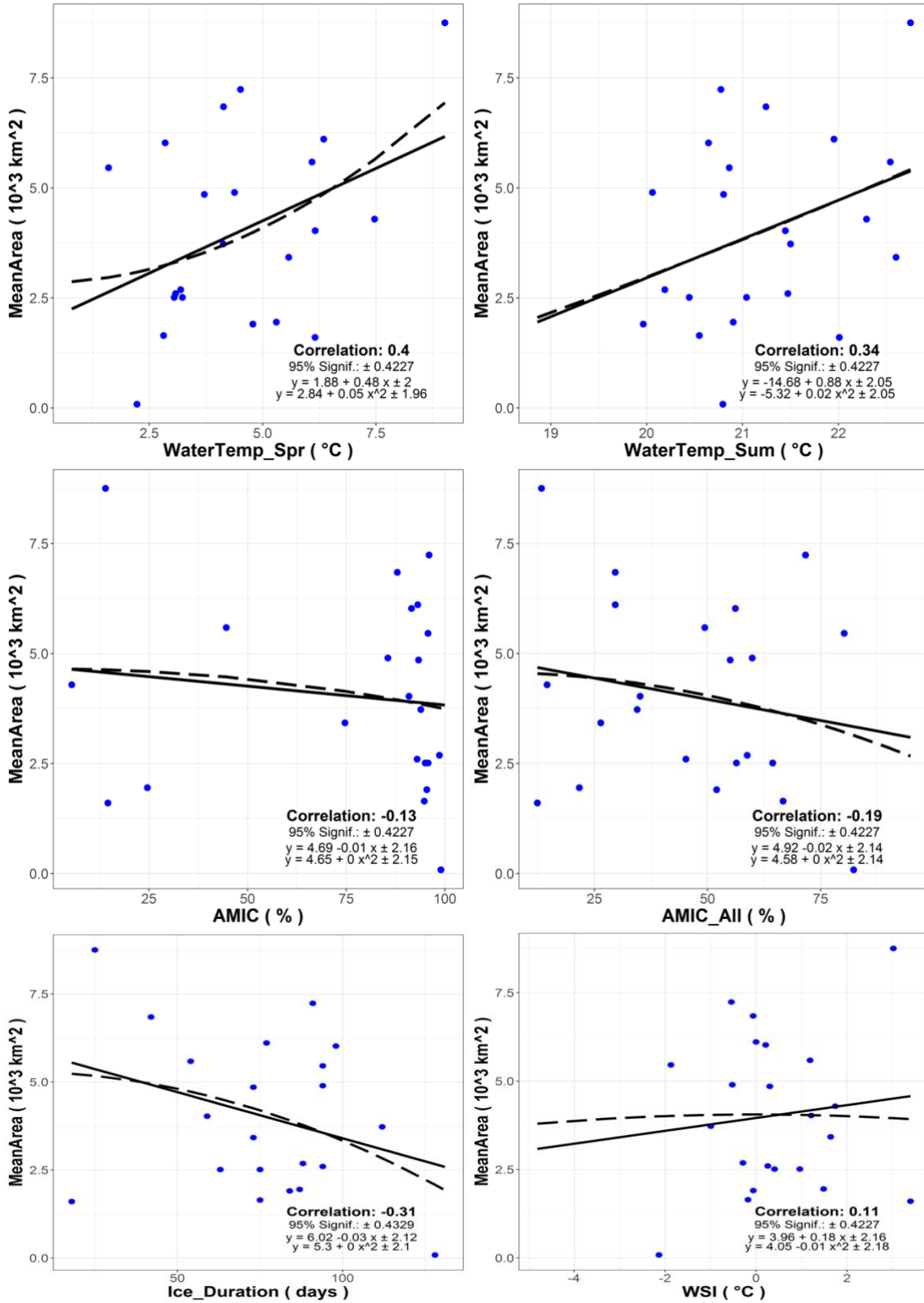


Figure 32. Regression between mean hypoxia area and other physical forcings.

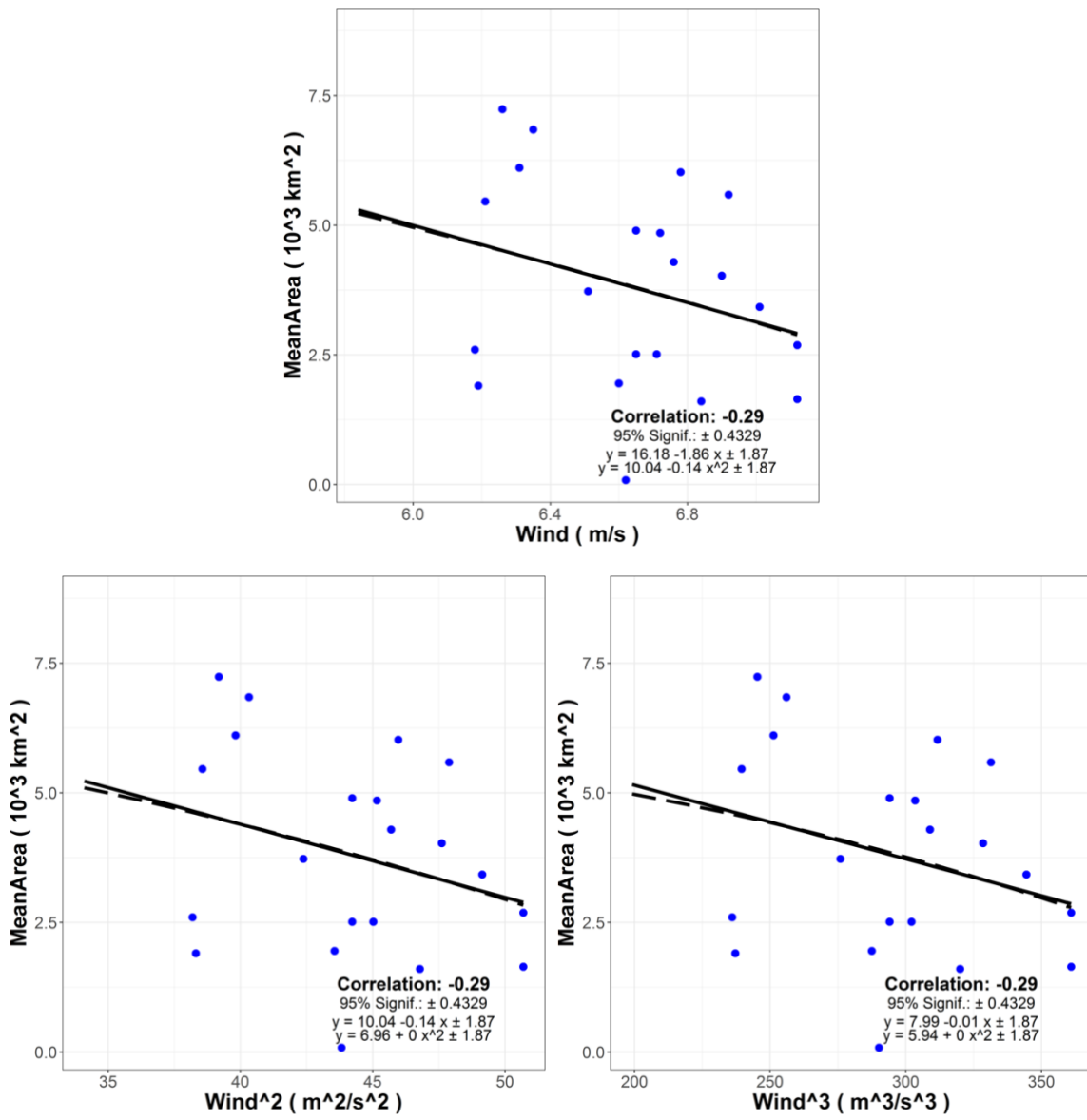


Figure 33. Regression between mean hypoxia area and wind speed, its quadratic and cubed forms.

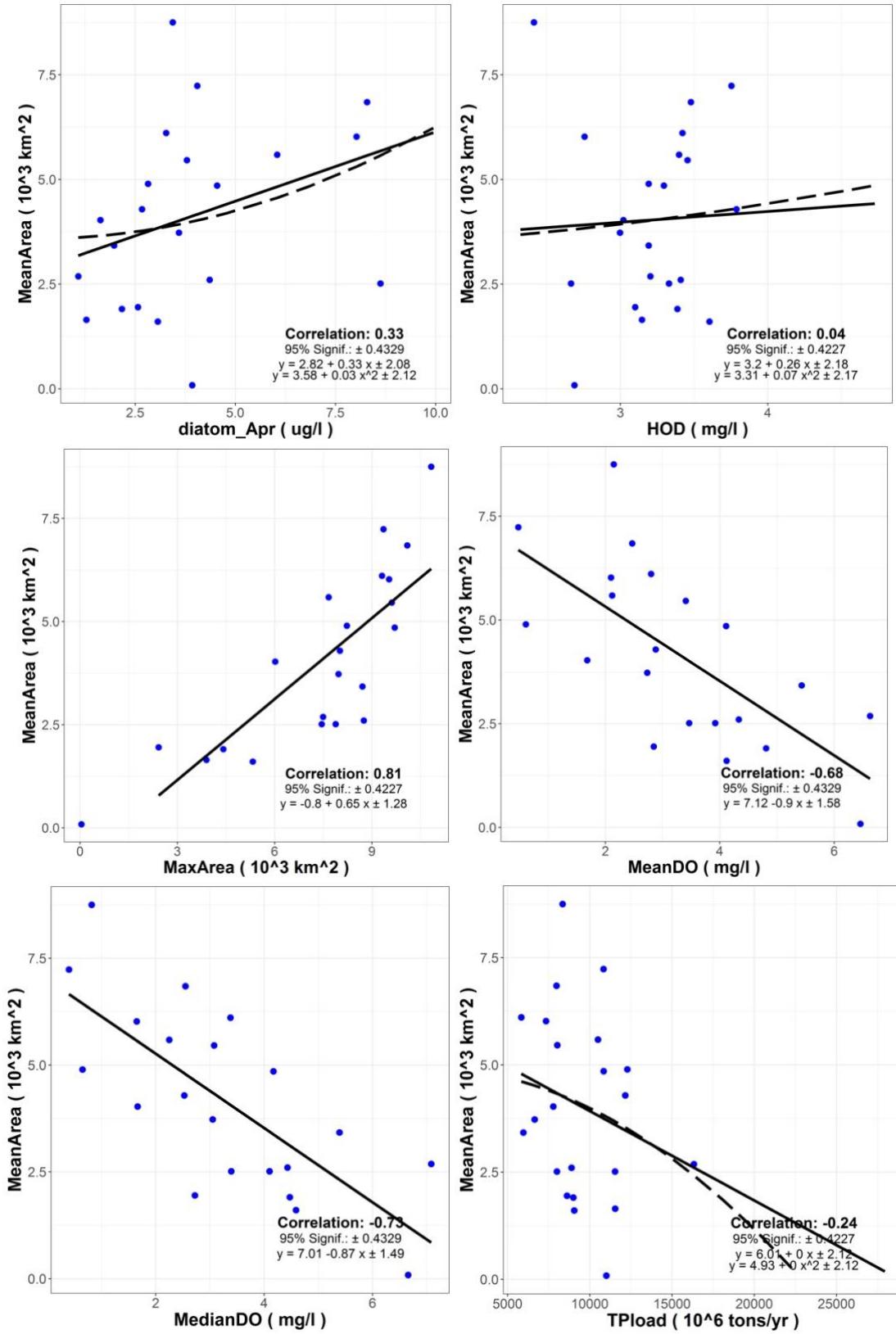


Figure 34. Regression between mean hypoxia area and other biological parameters.

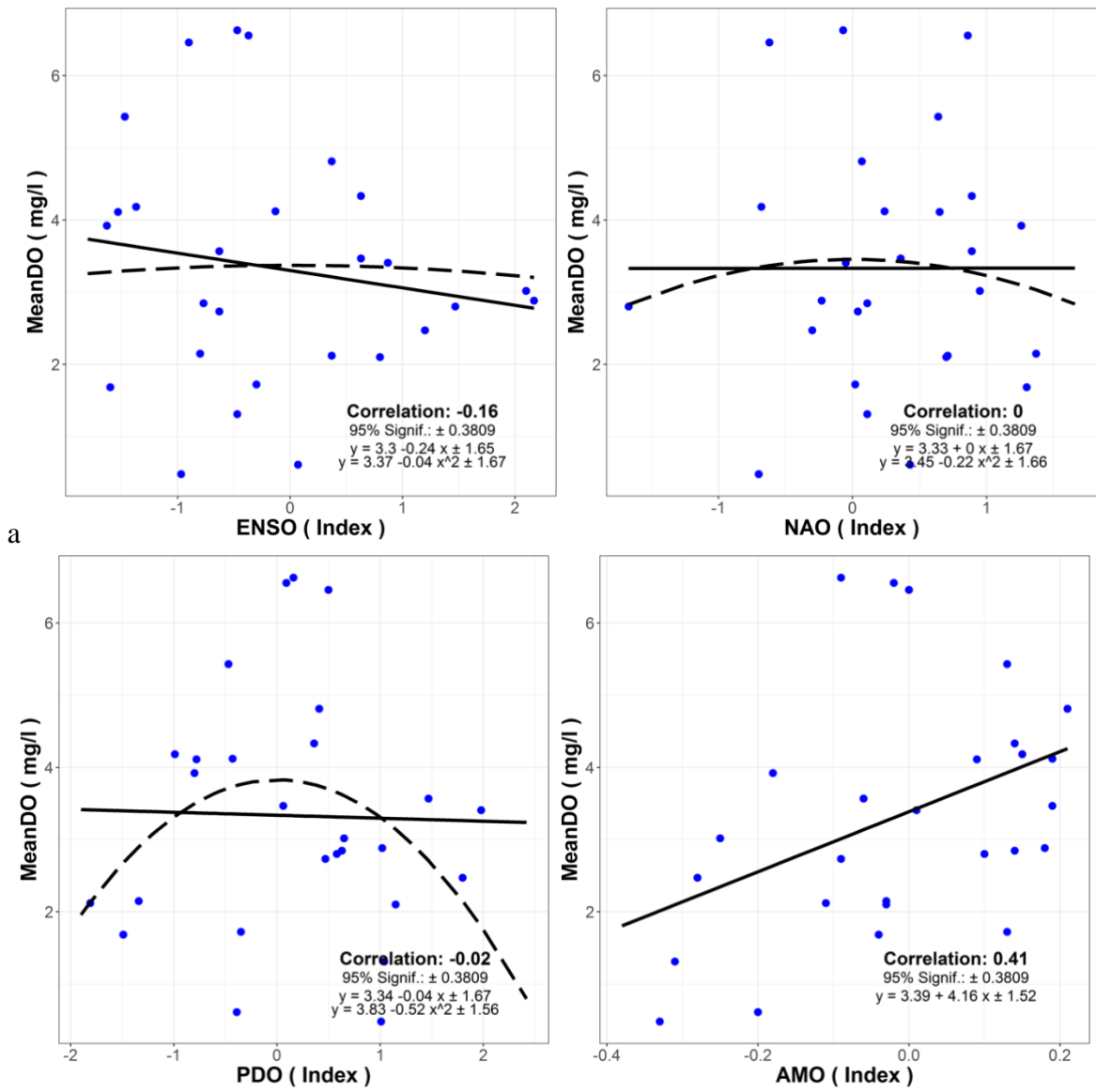


Figure 35. Regression between mean dissolved oxygen and four teleconnection patterns.

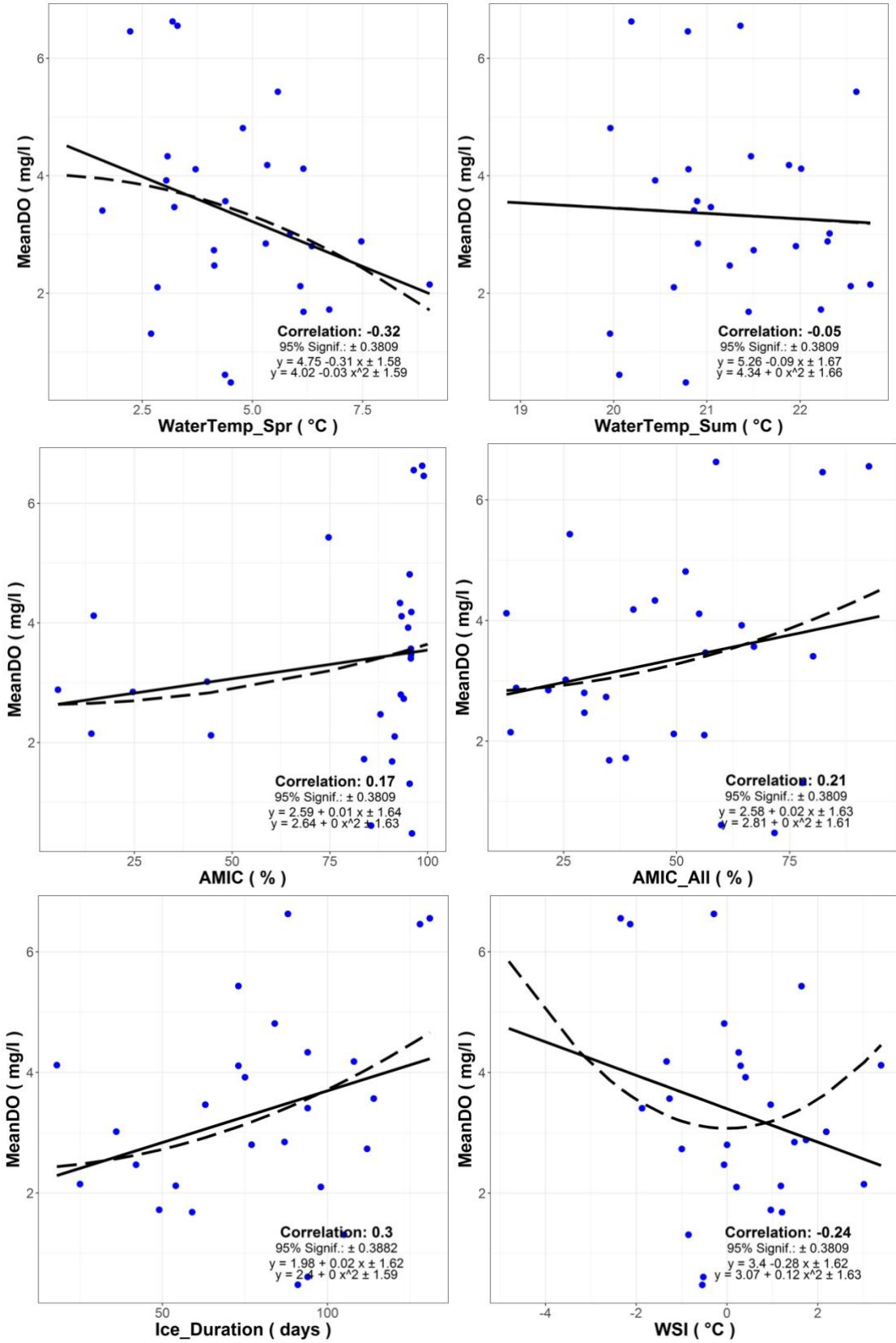


Figure 36. Regression between mean dissolved oxygen and other physical forcings.

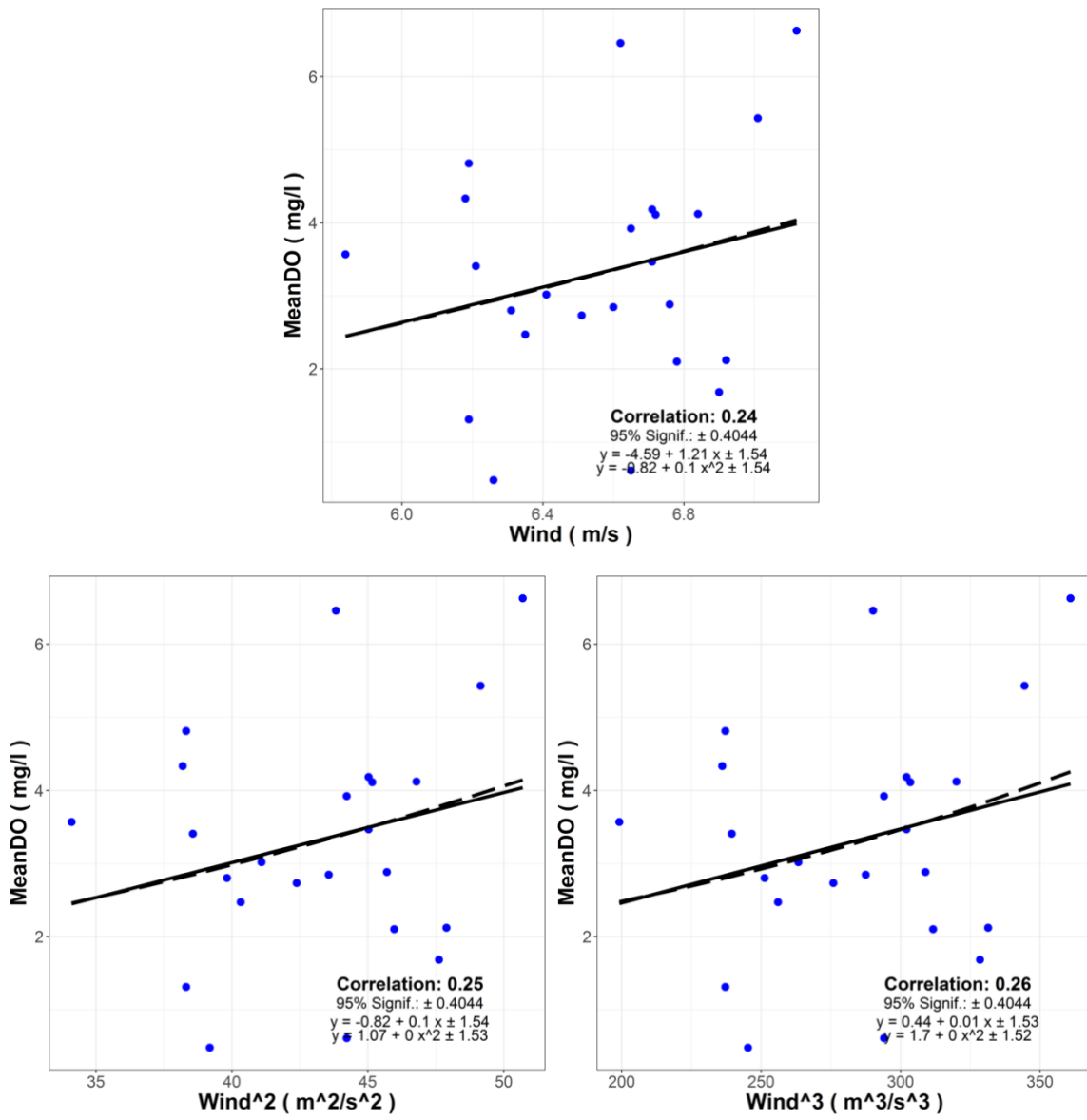


Figure 37. Regression between mean dissolved oxygen and wind speed, its quadratic and cubed forms.

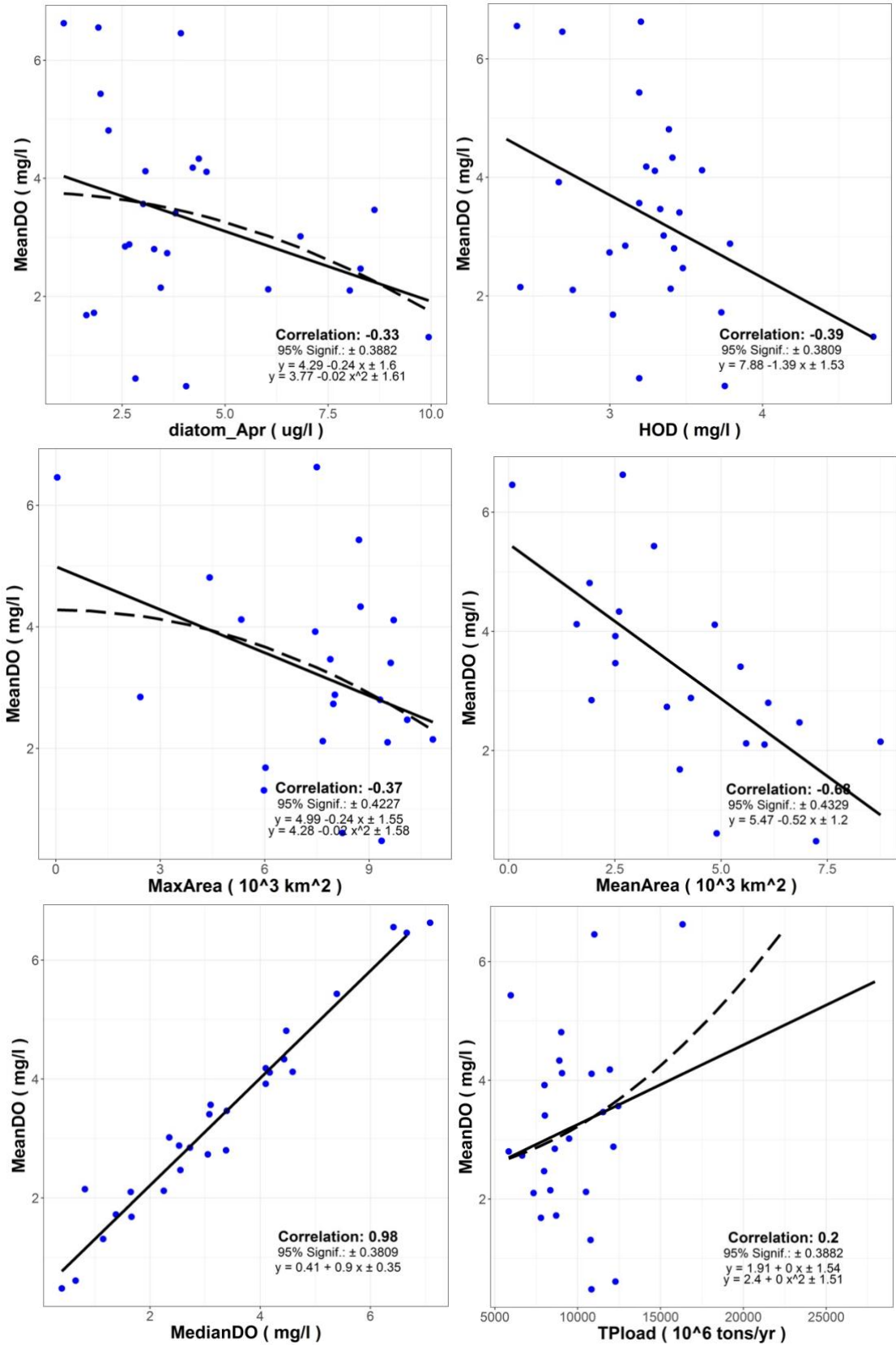


Figure 38. Regression between mean dissolved oxygen and other biological parameters.

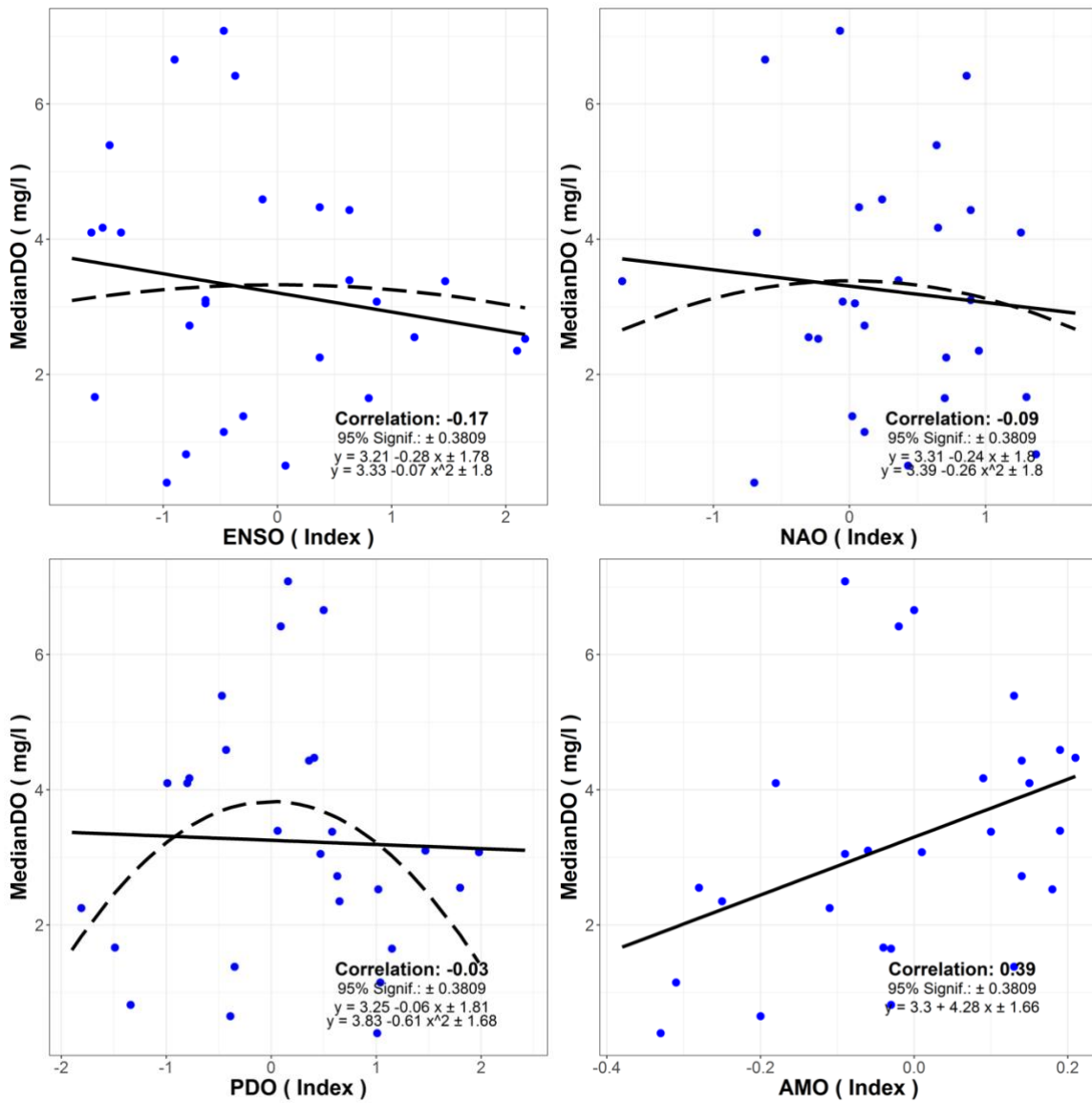


Figure 39. Regression between median dissolved oxygen and four teleconnection patterns.

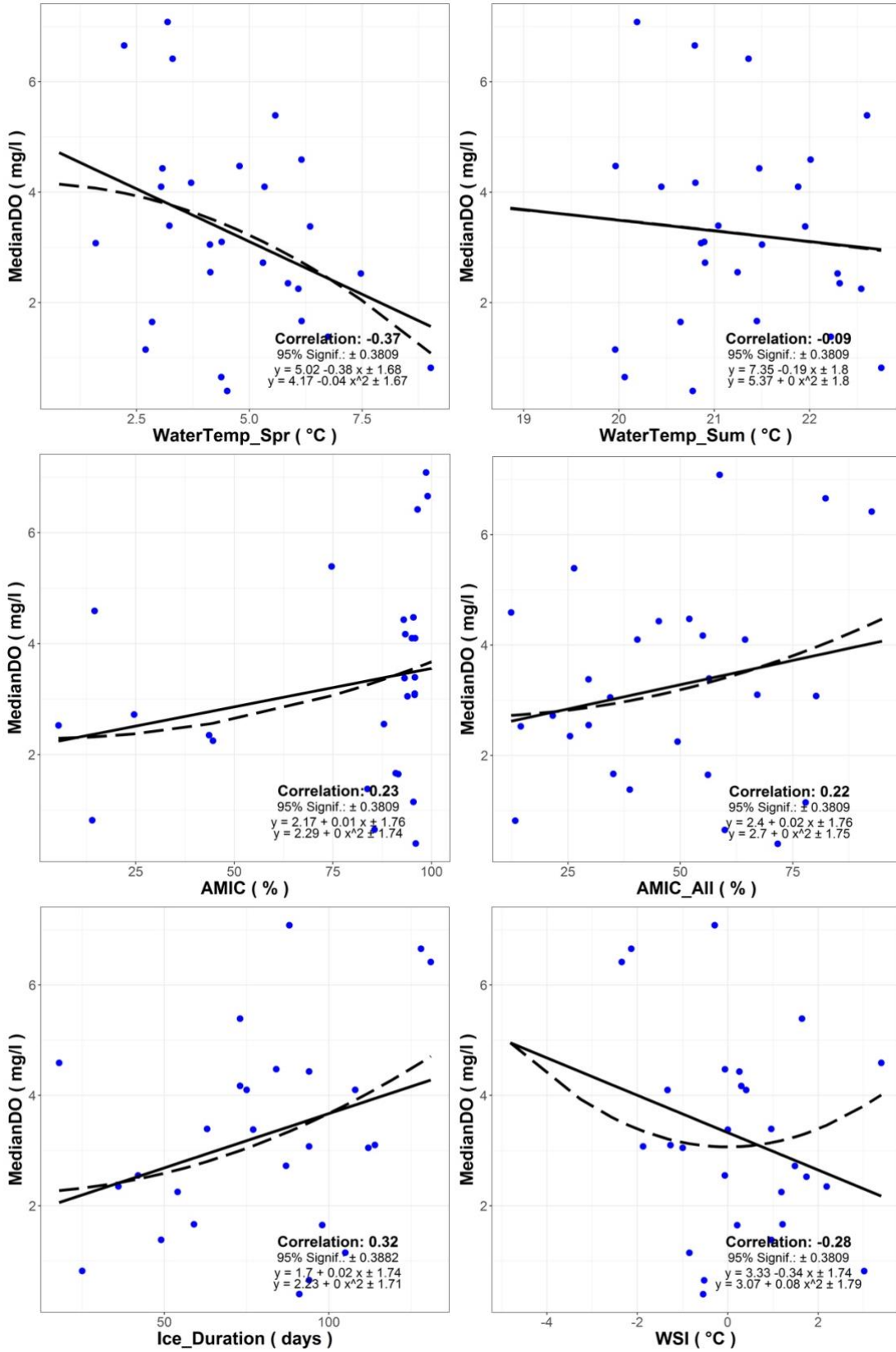


Figure 40. Regression between median dissolved oxygen and other physical forcings.

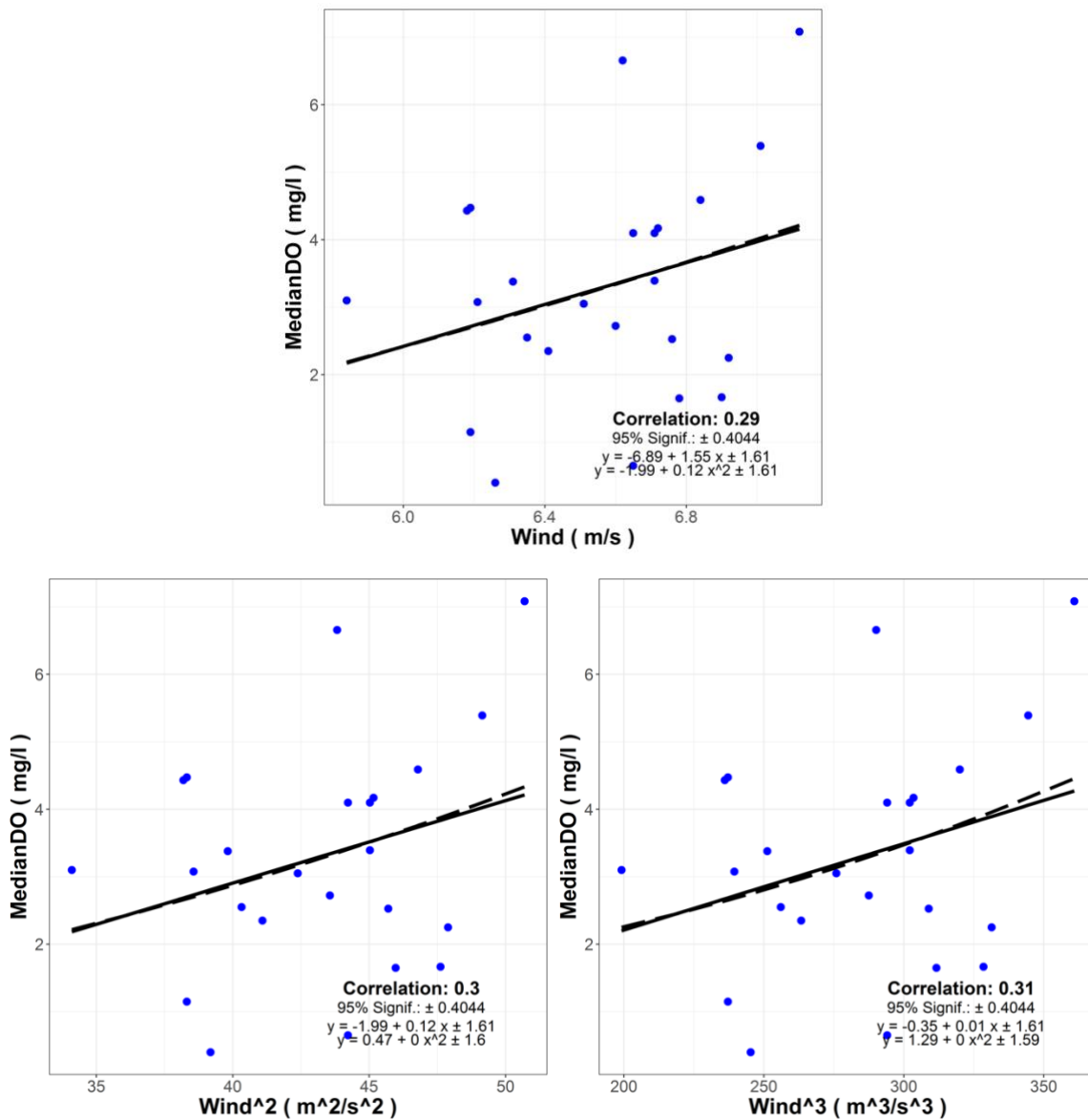


Figure 41. Regression between median dissolved oxygen and wind speed, its quadratic and cubed forms.

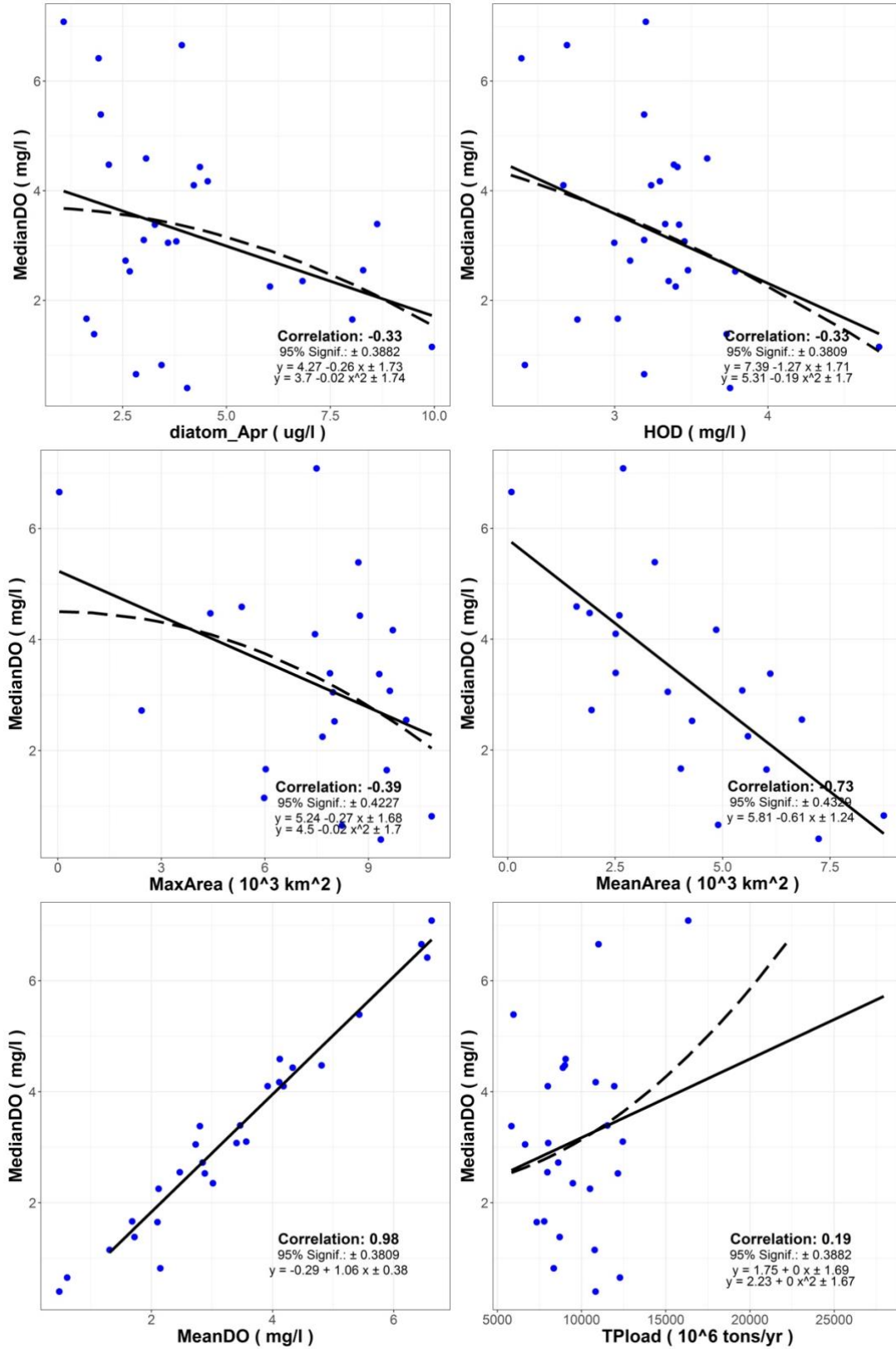


Figure 42. Regression between median dissolved oxygen and other biological parameters.

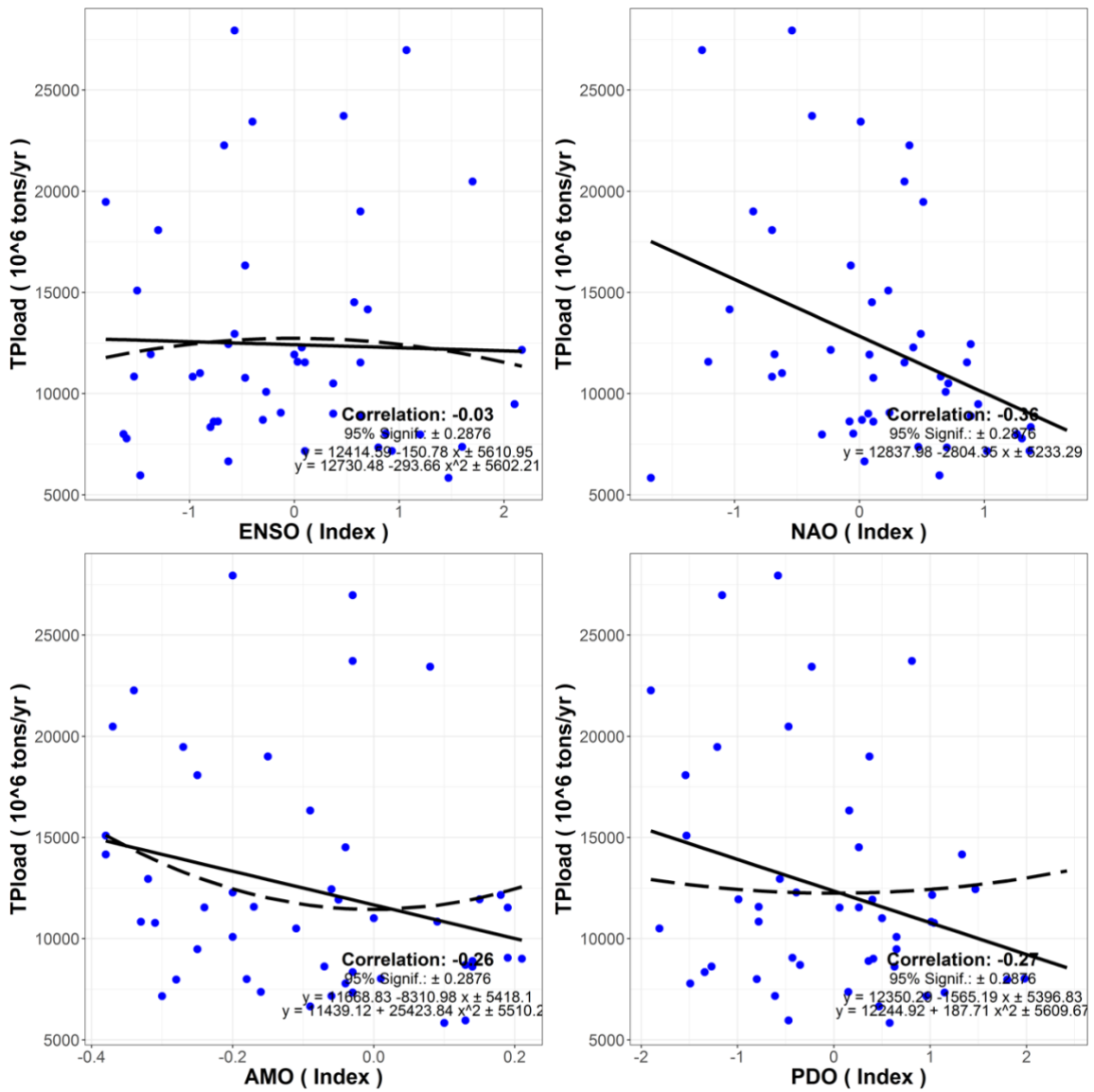


Figure 43. Regression between river phosphate load and four teleconnection patterns.

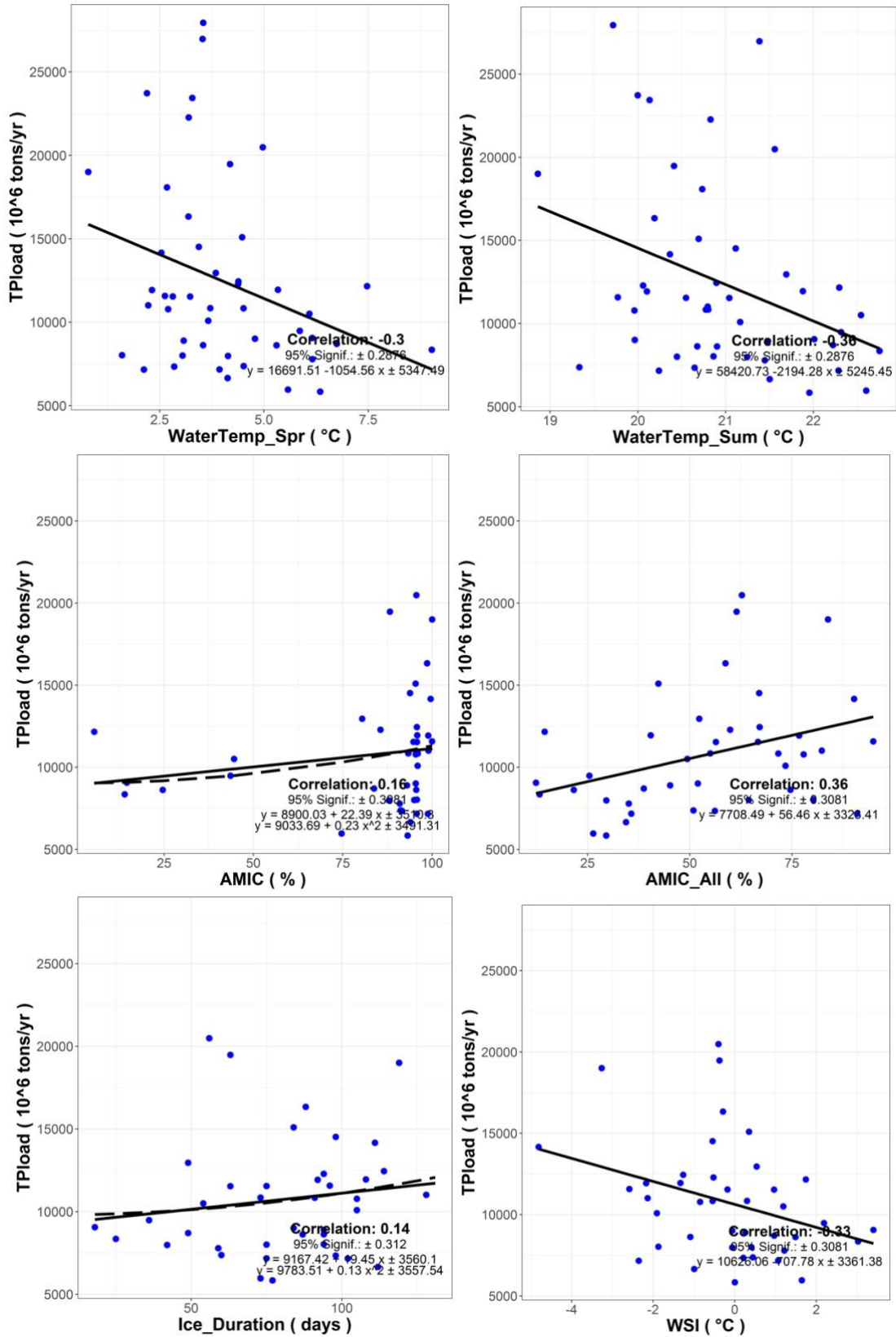


Figure 44. Regression between river phosphate load and other physical forcings.

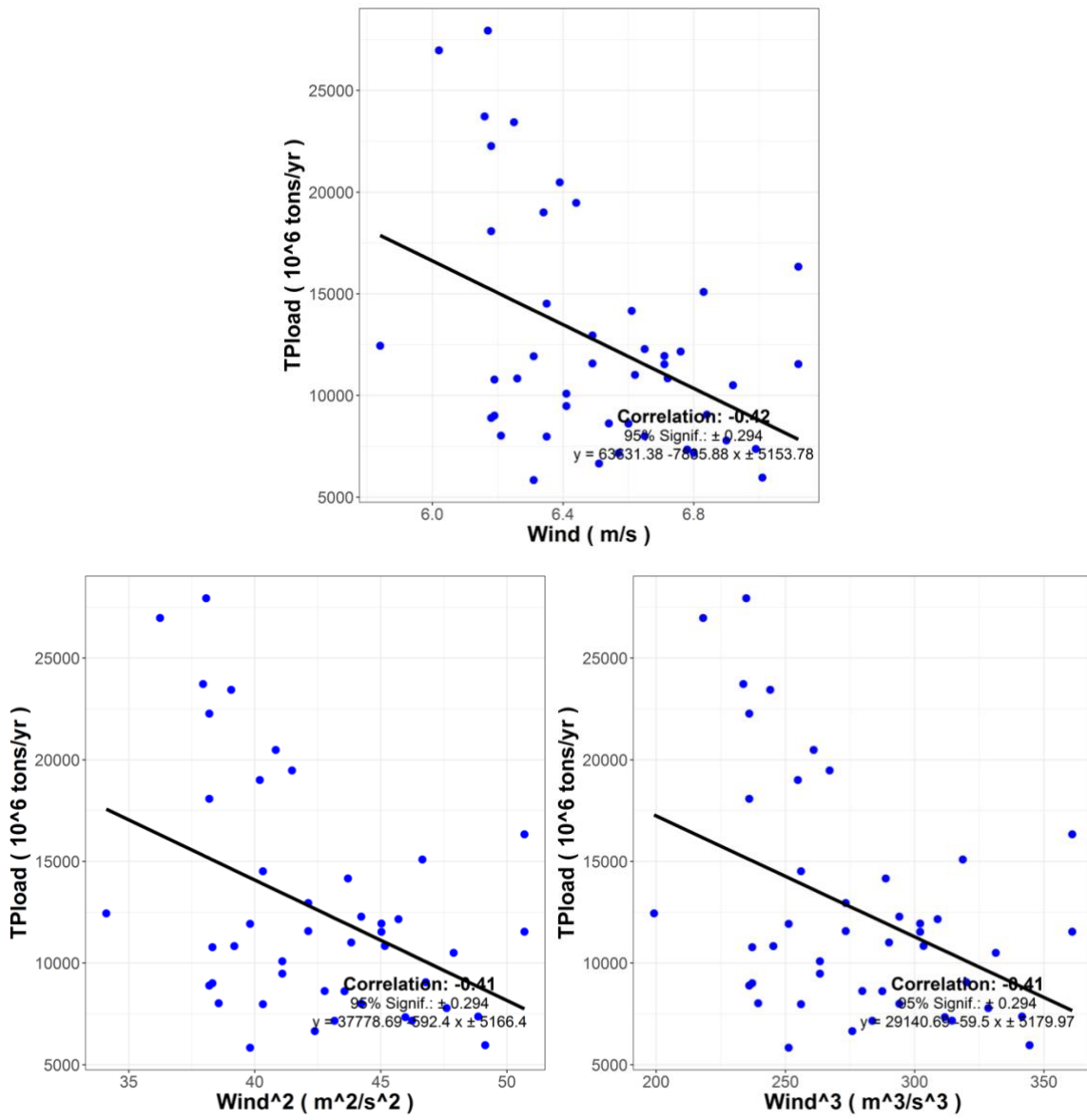


Figure 45. Regression between river phosphate load and wind speed, its quadratic and cubed forms.

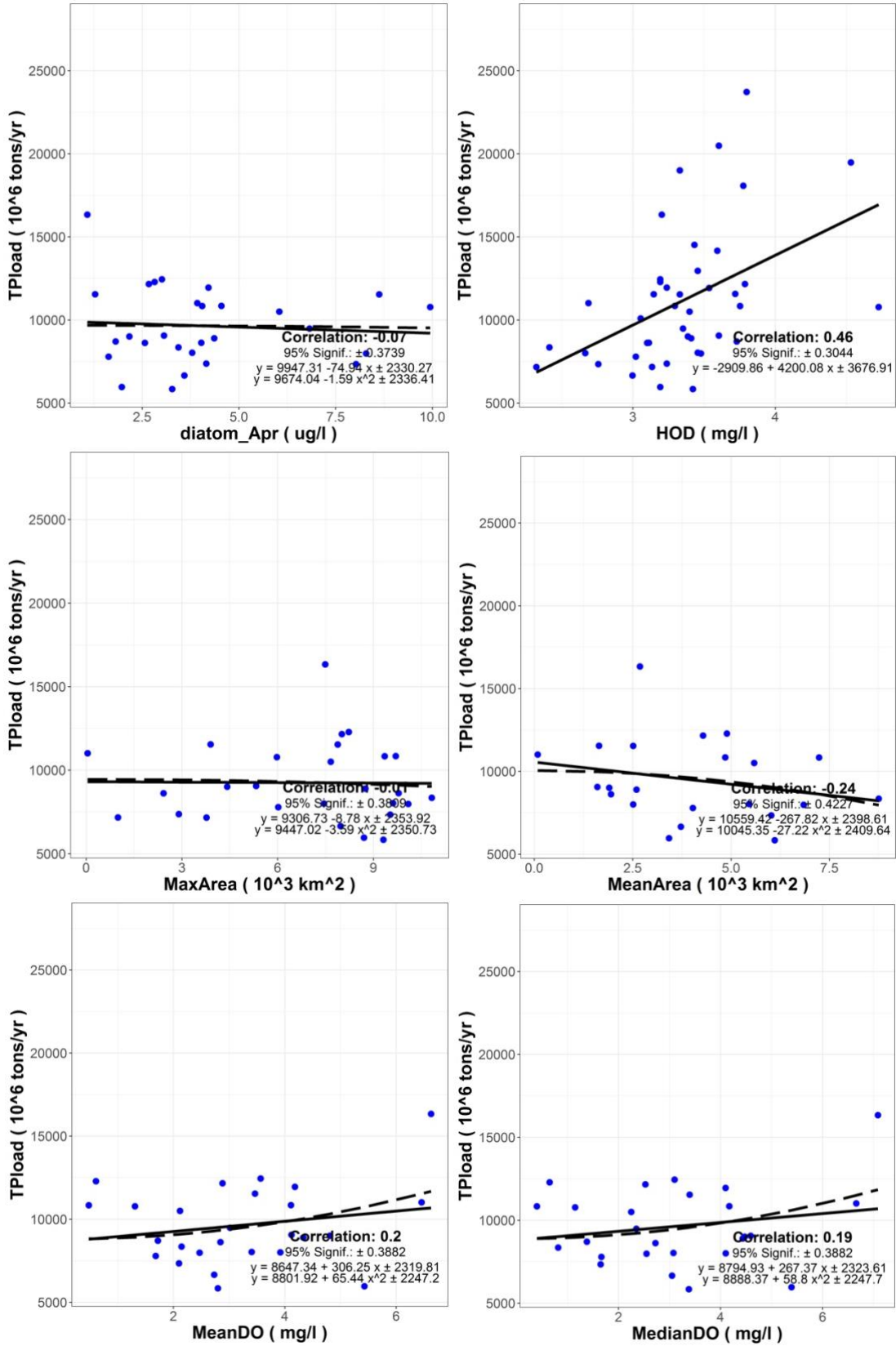


Figure 46. Regression between river phosphate load and other biological forcings.

5.0 SUMMARY

This technical memorandum provides preliminary analyses of Lake Erie biological parameters and the related physical/environmental forcings for the period 1970s-2010s. These linear regression scatters/graphs are quantitatively extracted into linear regression equations, which are easily used by a broad variety of users who, for various purposes, want to know what are the major forcings on Lake Erie ecosystems, based on the known observed AMIC, ice duration, teleconnection patterns, etc. Furthermore, this report reveals the relationships of teleconnection patterns and physical forcings to the biological parameters in Lake Erie via linear or/and non-linear manner. These comprehensive approaches can be further extracted to form multi-variable regression models to predict ecosystem change in the Great Lakes.

Based on the investigations above, the following summary can be drawn:

- 1) An individual teleconnection pattern (ENSO, PDO, NAO, or AMO) may have relationship with Great Lakes environmental parameters (AMIC, ice duration, WSI) and biological parameters via linear or/and non-linear manners. A weak correlation indicates that the teleconnection has no direct impact on an individual biological parameter.
- 2) Using a single environmental forcing, we can estimate or project a biological parameter using simple graphing and linear regression equation. The simple graphs and linear regressions are very practical and easy to use.
- 3) Multi-variable regression models may be next step to explore in-depth the biological parameters using physical/climate forcings as predictors.

6.0 ACKNOWLEDGMENTS

We appreciate Mr. Patrick Wang of Ann Arbor Huron High School for his summer project by volunteering his many hours to work on the data analysis using R-program. This is GLERL Contribution No. 1901 and CIGLR Contribution No. 1134.

7.0 REFERENCES

- Assel, R.A., and S. Rodionov. Atmospheric teleconnections for annual maximum ice cover on the Laurentian Great Lakes. *International Journal of Climatology* 18:425-442 (1998). <http://www.glerl.noaa.gov/pubs/fulltext/1998/19980001.pdf>
- Assel, R.A., F. H. Quinn, and C. E. Sellinger. Hydro-climatic factors of the recent drop in Laurentian Great Lakes water levels. *Bulletin of the American Meteorological Society* 85(8):1143-1151 (DOI: 10.1175/BAMS-85-8-1143) (2004b).
- Assel, R.A, J. Wang, A. Clites, and X. Bai. Analysis of Great Lakes ice cover climatology: Winters 2006-2011. NOAA Technical Memorandum GLERL-157. NOAA Great Lakes Environmental Research Laboratory, Ann Arbor, MI, 26 pp. (2013). https://www.glerl.noaa.gov/pubs/tech_reports/glerl-157/tm-157.pdf
- Bai, X., J. Wang, Q. Liu, D. Wang, and Y. Liu. Severe ice conditions in the Bohai Sea, China and mild ice conditions in the Great Lakes during the 2009/2010 winter: Links to El Nino and a strong negative Arctic Oscillation. *Journal of Applied Meteorology and Climatology* 50:1922-1935 (DOI:10.1175/2011JAMC2675.1) (2011).
- Bai, X., J. Wang, C.E. Sellinger, A.H. Clites, and R.A. Assel. Interannual variability of Great Lakes ice cover and its relationship to NAO and ENSO. *Journal of Geophysical Research* 117(C03002):25 pp. (DOI:10.1029/2010JC006932) (2012).
- Del Giudice, D., Y. Zhou, E. Sinha, A.M. Michalak. Long-Term Phosphorus Loading and Springtime Temperatures Explain Interannual Variability of Hypoxia in a Large Temperate Lake. *Environmental Science and Technology* 52:2046-2054. (DOI:10.1021/acs.est.7b04730) (2018).
- Dolan, D.M. and S.C. Chapra. Great Lakes total phosphorus revisited: 1. Loading analysis and update (1994-2008). *Journal of Great Lakes Research* 38:730-740 (DOI:10.1016/j.jglr.2012.10.001) (2012).
- Hu, H. and J. Wang. Modeling effects of tidal and wave mixing on circulation and thermohaline structures in the Bering Sea: Process studies, *Journal of Geophysical Research*, 115(C0100). (DOI:10.1029/2008JC005175) (2010).
- Hunter, T.S., A.H. Clites, A.D. Gronewold, and K.B. Campbell. Development and application of a North American Great Lakes hydrometeorological database - Part I: Precipitation, evaporation, runoff, and air temperature. *Journal of Great Lakes Research* 41(1):65-77 (DOI:10.1016/j.jglr.2014.4.12.006) (2015).
- Maccoux M.J., A. Dove, S.M. Backus, D.M. Dolan. Total and soluble reactive phosphorus loadings to Lake Erie: A detailed accounting by year, basin, country, and tributary. *Journal of Great Lakes Research* 42:1151-1165 (DOI:10.1016/j.jglr.2016.08.005) (2016).

- Michalak A. M., et al. Record-setting algal bloom in Lake Erie caused by agricultural and meteorological trends consistent with expected future conditions. *Proceedings of the National Academy of Sciences* 110(16):6448-6452 (DOI: 0.1073/pnas.1216006110) (2013).
- Mishra, V., K. Cherkauer, C. Bowling, and M. Huber. Lake Ice phenology of small lakes: Impacts of climate variability in the Great Lakes region. *Global and Planetary Change* 76(3-4):166-185 (DOI:10.1016/j.gloplacha.2011.01.004) (2011)
- Niimi, A.J. Economic and environmental issues of the proposed extension of the winter navigation season and improvements on the Great Lakes-St. Lawrence Seaway system, *Journal of Great Lakes Research* 8:532–549 (1982).
- Scavia D, et al. Assessing and addressing the re-eutrophication of Lake Erie: Central basin hypoxia. *Journal of Great Lakes Research* 40(2):226-246 (DOI:10.1016/j.jglr.2014.02.004) (2014).
- Vanderploeg, H.A., S.J. Bolsenga, G.L. Fahnenstiel, J.R. Liebig, and W.S. Gardner. Plankton ecology in an ice-covered bay of Lake Michigan: utilization of a winter phytoplankton bloom by reproducing copepods. *Hydrobiologia* 243/244:175-183 (1992).
- Wang, J., R.A. Assel, S. Walterscheid, A.H. Clites, and X. Bai. Great Lakes ice climatology update: Winter 2006-2011. Description of the digital ice cover dataset. NOAA Technical Memorandum GLERL-155. NOAA, Great Lakes Environmental Research Laboratory, Ann Arbor, MI, 37 pp. (2012). https://www.glerl.noaa.gov/pubs/tech_reports/glerl-155/tm-155.pdf
- Wang, J., J. Kessler, F. Hang, H. Hu, A.H. Clites, and P. Chu. Analysis of Great Lakes Ice Cover Climatology: Winters 2012-2017. NOAA Technical Memorandum GLERL-171. NOAA, Great Lakes Environmental Research Laboratory, Ann Arbor, MI, 25 pp. (2017). https://www.glerl.noaa.gov/pubs/tech_reports/glerl-171/tm-171.pdf
- Wang, J., J. Kessler, F. Hang, H. Hu, A.H. Clites, and P. Chu. Great Lakes Ice Climatology Update of Winters 2012-2017: Seasonal Cycle, Interannual Variability, Decadal Variability, and Trend for the period 1973-2017. NOAA Technical Memorandum GLERL-170. NOAA, Great Lakes Environmental Research Laboratory, Ann Arbor, MI (2017). https://www.glerl.noaa.gov/pubs/tech_reports/glerl-170/tm-170.pdf
- Wang, J., J. Kessler, X. Bai, A.H. Clites, B.M. Lofgren, A. Assuncao, J.F. Bratton, P. Chu, and G.A. Leshkevich. Decadal variability of Great Lakes ice cover in response to AMO and PDO, 1963-2017. *Journal of Climate* 31(18):7249-7268 (DOI:10.1175/JCLI-D-17-0283.1) (2018).
- Watson, S.B. et al. The re-eutrophication of Lake Erie: Harmful algal blooms and hypoxia. *Harmful Algae* 56:44-66. (DOI: 10.1016/j.hal.2016.04.010) (2016).
- Zhou, Y., A.M. Michalak, D. Beletsky, Y.R. Rao, and R.P. Richards. Record-breaking Lake Erie hypoxia during 2012 drought. *Environmental Science and Technology* 49(2):800-807 (DOI:10.1021/es503981n) (2015).

8.0 APPENDIX: LAKE ERIE BIOLOGICAL PARAMETERS AND ENVIRONMENTAL FORCINGS

This appendix provides original data in a format of table to the users who may use them for their purposes. These data include the biological data and the environmental forcings, including four teleconnection pattern indices

Tables 5 and 6 summarize the above-analyzed statistics information for these biological and environmental parameters.

Table 7 summarizes the long-term trend of each parameters and some important statistics of the long-term changes.

Table 3. Time series of biological parameters.

Year	diatom_Apr (ug/l)	HOD (mg/l)	MaxArea (10 ³ km ²)	MeanArea (10 ³ km ²)	MeanDO (mg/l)	MedianDO (mg/l)	Tpload (10 ⁶ tons/yr)
1967	NA	NA	NA	NA	NA	NA	23437.000
1968	NA	NA	NA	NA	NA	NA	27944.000
1969	NA	NA	NA	NA	NA	NA	26977.000
1970	NA	3.799	NA	NA	NA	NA	23724.000
1971	NA	3.776	NA	NA	NA	NA	18077.000
1972	NA	NA	NA	NA	NA	NA	22271.000
1973	NA	3.604	NA	NA	NA	NA	20485.000
1974	NA	4.531	NA	NA	NA	NA	19476.424
1975	NA	3.455	NA	NA	NA	NA	12952.485
1976	NA	NA	NA	NA	NA	NA	15093.917
1977	NA	3.593	NA	NA	NA	NA	14161.403
1978	NA	3.330	NA	NA	NA	NA	19003.880
1979	NA	3.719	NA	NA	NA	NA	11569.713
1980	NA	3.432	NA	NA	NA	NA	14518.691
1981	NA	3.055	NA	NA	NA	NA	10085.430
1982	NA	3.535	NA	NA	NA	NA	11924.235
1983	6.828	3.352	NA	NA	3.017	2.350	9482.416
1984	3.010	3.192	NA	NA	3.567	3.100	12445.663
1985	4.052	3.753	9.357	7.235	0.480	0.400	10833.868
1986	9.943	4.725	5.978	NA	1.310	1.150	10778.303
1987	8.289	3.478	10.094	6.845	2.470	2.550	7977.291
1988	8.026	2.757	9.531	6.022	2.100	1.650	7341.992
1989	NA	2.666	7.451	2.513	3.920	4.100	8002.050
1990	2.822	3.192	8.231	4.895	0.610	0.650	12283.098
1991	6.046	3.398	7.668	5.588	2.120	2.250	10499.543
1992	4.158	3.238	2.903	NA	NA	NA	7369.139
1993	1.283	3.146	3.899	1.646	NA	NA	11542.919
1994	NA	2.323	3.769	NA	NA	NA	7159.000
1995	NA	3.135	0.996	NA	NA	NA	7171.000
1996	3.925	2.689	0.043	0.087	6.458	6.659	11010.000
1997	1.081	3.204	7.495	2.686	6.627	7.084	16333.000
1998	2.672	3.787	8.014	4.289	2.881	2.527	12158.000
1999	1.973	3.192	8.708	3.422	5.431	5.391	5963.000
2000	1.632	3.021	6.022	4.029	1.683	1.665	7782.000
2001	3.592	2.998	7.971	3.726	2.732	3.050	6651.000
2002	3.065	3.604	5.329	1.603	4.120	4.590	9059.000
2003	3.792	3.455	9.617	5.458	3.407	3.077	8024.224
2004	2.168	3.387	4.419	1.906	4.810	4.474	9005.699
2005	4.361	3.410	8.751	2.599	4.332	4.433	8892.290

2006	2.569	3.101	2.426	1.949	2.846	2.724	8616.810
2007	8.624	3.330	7.884	2.513	3.465	3.393	11537.527
2008	4.546	3.295	9.704	4.852	4.111	4.171	10843.113
2009	4.028	3.112	9.791	NA	NA	NA	8623.343
2010	3.275	3.421	9.314	6.108	2.800	3.380	5839.478
2011	4.214	3.238	NA	NA	4.182	4.100	11945.986
2012	3.437	2.414	10.830	8.751	2.147	0.819	8349.978
2013	1.815	3.730	NA	NA	1.722	1.381	8700.954
2014	1.922	2.391	NA	NA	6.555	6.419	NA
2015	4.791	NA	NA	NA	NA	NA	NA

Table 4. Time series of teleconnection pattern indices.

Year	ENSO (°C)	NAO	AMO (°C)	PDO (°C)	Year	ENSO (°C)	NAO	AMO (°C)	PDO (°C)
1951	-0.70	-0.08	0.07	-1.12	1985	-0.97	-0.70	-0.33	1.01
1952	0.57	0.47	0.18	-1.38	1986	-0.47	0.11	-0.31	1.04
1953	0.37	-0.20	0.27	-0.20	1987	1.20	-0.30	-0.28	1.80
1954	0.70	0.21	0.20	-0.95	1988	0.80	0.70	-0.03	1.15
1955	-0.67	-0.76	0.02	-0.61	1989	-1.63	1.26	-0.18	-0.80
1956	-1.13	-0.39	0.18	-2.66	1990	0.07	0.43	-0.20	-0.39
1957	-0.17	0.42	-0.05	-1.26	1991	0.37	0.71	-0.11	-1.81
1958	1.73	-0.49	0.11	0.11	1992	1.60	0.47	-0.16	0.15
1959	0.60	-0.30	0.15	0.37	1993	0.10	0.86	-0.24	0.26
1960	-0.07	-0.91	0.17	0.29	1994	0.10	1.02	-0.30	0.96
1961	0.03	0.31	0.09	0.59	1995	0.93	1.36	-0.06	-0.61
1962	-0.20	-0.11	0.17	-1.71	1996	-0.90	-0.62	0.00	0.50
1963	-0.33	-1.47	0.17	-0.48	1997	-0.47	-0.07	-0.09	0.16
1964	1.00	-1.43	-0.04	-0.43	1998	2.17	-0.23	0.18	1.02
1965	-0.57	-0.61	-0.17	-1.31	1999	-1.47	0.64	0.13	-0.47
1966	1.43	-0.59	-0.06	-0.26	2000	-1.60	1.30	-0.04	-1.49
1967	-0.40	0.01	0.08	-0.23	2001	-0.63	0.04	-0.09	0.47
1968	-0.57	-0.54	-0.20	-0.58	2002	-0.13	0.24	0.19	-0.43
1969	1.07	-1.26	-0.03	-1.16	2003	0.87	-0.05	0.01	1.98
1970	0.47	-0.38	-0.03	0.81	2004	0.37	0.07	0.21	0.41
1971	-1.30	-0.70	-0.25	-1.54	2005	0.63	0.89	0.14	0.36
1972	-0.67	0.40	-0.34	-1.90	2006	-0.77	0.11	0.14	0.63
1973	1.70	0.36	-0.37	-0.47	2007	0.63	0.36	0.19	0.06
1974	-1.80	0.51	-0.27	-1.21	2008	-1.53	0.65	0.09	-0.78
1975	-0.57	0.49	-0.32	-0.56	2009	-0.73	-0.08	-0.07	-1.27
1976	-1.50	0.23	-0.38	-1.53	2010	1.47	-1.67	0.10	0.58
1977	0.70	-1.04	-0.38	1.33	2011	-1.37	-0.68	0.15	-0.99
1978	0.63	-0.85	-0.15	0.37	2012	-0.80	1.37	-0.03	-1.34
1979	0.03	-1.21	-0.17	-0.78	2013	-0.30	0.02	0.13	-0.35
1980	0.57	0.10	-0.04	0.26	2014	-0.37	0.86	-0.02	0.09
1981	-0.27	0.69	-0.20	0.65	2015	0.63	1.66	0.02	2.42
1982	0.00	0.08	-0.05	0.40	2016	2.43	1.31	0.21	1.43
1983	2.10	0.95	-0.25	0.65	2017	-0.33	0.65	0.26	0.88
1984	-0.63	0.89	-0.06	1.47	2018	-0.90	1.30	0.20	0.52

Table 5. Correlation coefficients between environmental/physical forcings and biological parameters. The bolded coefficients are at the 95% significance level.

	Diatom	HOD	Max area	Mean area	Mean DO	Median DO	TPLoad
ENSO	0.32	0.09	-0.02	0.19	-0.16	-0.17	-0.03
ENSO ²	0.04	0.16	0.14	0.16	-0.03	-0.05	-0.06
NAO	0.0	-0.41	-0.13	-0.04	0.0	-0.09	-0.36
NAO ²	-0.09	-0.33	0.01	0.33	-0.09	-0.1	-0.19
PDO	-0.26	-0.05	-0.01	0.03	-0.02	-0.03	-0.27
PDO ²	-0.25	0.11	0.4	0.58	-0.34	-0.37	0.03
AMO	-0.31	-0.16	0.02	-0.37	0.41	0.39	-0.26
AMO ²	-0.39	-0.39	-0.04	-0.12	0.43	0.40	-0.19
AMIC	0.11	-0.01	-0.14	-0.19	0.21	0.22	0.36
Ice duration	-0.08	-0.17	-0.21	-0.31	0.30	0.32	0.14
Wind speed	-0.27	-0.36	-0.25	-0.29	-0.24	-0.29	-0.42
T_w@spr	-0.25	-0.03	0.22	0.4	-0.32	-0.37	-0.30
T_w@sum	-0.08	-0.14	0.25	0.34	-0.05	-0.09	-0.36
WSI	-0.02	0.0	0.11	0.11	-0.24	-0.28	-0.33

Table 6. Correlation coefficients between biological parameters. The bolded coefficients are at the 95% significance level.

	Diatom	HOD	Max area	Mean area	Mean DO	Median DO	TPLoad
Diatom		0.35	0.23	0.33	-0.33	-0.33	-0.07
HOD			0.13	0.04	-0.39	-0.33	0.46
Max area				0.81	-0.37	-0.39	-0.01
Mean area					-0.68	-0.73	-0.24
Mean DO						0.98	0.20
Median DO							0.19
TPLoad							

Table 7. Summary of the long-term trend [$y=a+b(t-T_0)$, where t is time in year] of each parameter and some important statistics of the long-term changes.

	a	b (annual chn)	T₀ (yrs)	Abso. Decadal Chn	Relat. Decadal chn (%)	Abso. total chn	Relat. total chn (%)	Mean	STD	STD/ Mean
diatom_Apr (ug/l)	5.424	-0.082	1983	-0.817	-20.109	-2.697	-66.358	4.065	2.279	0.561
HOD (mg/l)		-0.015	1970	-0.154	-4.633	-0.693	-20.850	3.325	0.471	0.142
MaxArea (10 ³ km ²)	6.077	0.063	1985	0.628	9.107	1.759	25.501	6.896	2.961	0.429
MeanArea (10 ³ km ²)	4.378	-0.025	1985	-0.252	-6.252	-0.706	-17.506	4.033	2.178	0.540
MeanDO (mg/l)	2.464	0.055	1983	0.546	16.402	1.748	52.487	3.330	1.667	0.501
MedianDO (mg/l)	2.375	0.055	1983	0.547	16.871	1.750	53.986	3.242	1.807	0.557
TPload (10 ⁶ tons/yr)	19436.361	-304.89	1967	-3048.90	-24.541	-14329.83	-115.341	12423.891	5613.100	0.452
Wind (m/s)	6.297	0.010	1967	0.098	1.505	0.441	6.775	6.513	0.303	0.047
WaterTemp_ Spr (°C)	2.925	0.047	1967	0.473	11.641	2.315	57.043	4.059	1.599	0.394
WaterTemp_ Sum (°C)	20.337	0.027	1967	0.271	1.293	1.330	6.335	20.988	0.901	0.043
IceDuration (days)	83.116	-0.039	1973	-0.386	-0.469	-1.658	-2.015	82.310	26.896	0.327
AMIC (%)	92.451	-0.399	1973	-3.986	-4.741	-17.139	-20.384	84.081	25.450	0.303
AMIC_All (%)	66.871	-0.523	1973	-5.231	-9.360	-22.492	-40.246	55.887	23.296	0.417
FDD (days)	75.726	-0.171	1973	-1.708	-2.368	-7.344	-10.180	72.140	14.300	0.198
WSI (°C)	-1.007	0.034	1973	0.337	112.950	1.451	485.685	-0.299	1.669	5.588
WSI_GLERL (°C)	-3.073	0.038	1973	0.383	16.881	1.647	72.590	-2.268	1.918	0.846